ENRICHMENT OF CELL CYCLE PHASES OF SYNCHRONIZED ESTROGEN RECEPTOR-POSITIVE CELL MODELS DERIVED FROM BREAST ADENOCARCINOMAS

A THESIS SUBMITTED TO
THE GRADUATE SCHOOL OF NATURAL AND APPLIED SCIENCES
OF
MIDDLE EAST TECHNICAL UNIVERSITY

BY

PELİN TOKER

IN PARTIAL FULFILLMENT OF THE REQUIREMENTS
FOR
THE DEGREE OF MASTER OF SCIENCE
IN
MOLECULAR BIOLOGY AND GENETICS

AUGUST 2024

Approval of the thesis:

ENRICHMENT OF CELL CYCLE PHASES OF SYNCHRONIZED ESTROGEN RECEPTOR-POSITIVE CELL MODELS DERIVED FROM BREAST ADENOCARCINOMAS

submitted by **PELİN TOKER** in partial fulfillment of the requirements for the degree of **Master of Science** in **Molecular Biology and Genetics, Middle East Technical University** by,

Prof. Dr. Naci Emre Altun
Dean, **Graduate School of Natural and Applied Sciences** _____

Prof. Dr. Mesut Muyan
Head of the Department, **Biological Sciences** _____

Prof. Dr. Mesut Muyan
Supervisor, **Biological Sciences, METU** _____

Examining Committee Members:

Prof. Dr. Ayşe Elif Erson Bensan
Biological Sciences, METU _____

Prof. Dr. Mesut Muyan
Biological Sciences, METU _____

Assist. Prof. Dr. Bahar Değirmenci Uzun
Molecular Biology and Genetics, Bilkent University _____

Date: 27.08.2024

I hereby declare that all information in this document has been obtained and presented in accordance with academic rules and ethical conduct. I also declare that, as required by these rules and conduct, I have fully cited and referenced all material and results that are not original to this work.

Name Last name : Pelin Toker

Signature :

ABSTRACT

ENRICHMENT OF CELL CYCLE PHASES OF SYNCHRONIZED ESTROGEN RECEPTOR-POSITIVE CELL MODELS DERIVED FROM BREAST ADENOCARCINOMAS

Toker, Pelin
Master of Science, Molecular Biology and Genetics
Supervisor: Prof. Dr. Mesut Muyan

August 2024, 69 pages

17β-estradiol (E2), the main circulating estrogen hormone, is a critical signaling factor for the growth, differentiation, and function of the breast tissue. The effects of E2 on the breast tissue are primarily mediated by the estrogen receptor α (ERα) and deregulation of the E2-ERα signaling contributes to the initiation/progression of breast cancer and resistance to treatments. Breast cancer cell lines as in vitro model systems provide invaluable insight into cellular events, drug discovery, and drug resistance. Among ERα-synthesizing cell lines, MCF7 and T47D cells are widely used to elucidate cell cycle phase-specific molecular events that coordinate cellular proliferation mediated by E2-ERα. Due to variable results in generating phase-enriched populations with various approaches, we wanted to reassess cell cycle synchronization-coupled phase enrichment with charcoal dextran-treated fetal bovine serum, CD-FBS, as an effective hormone withdrawal approach, alone or in combination with excess thymidine, as a DNA replication inhibitor, and/or nocodazole, a microtubule poison, in MCF7 and T47D cells. We find that hormone withdrawal synchronizes both MCF7 and T47D cells at the G0/G1 phase. Supplementation of CD-FBS with E2 enriches the S phase population and together with nocodazole and nocodazole-coupled mitotic shake-off augments the G2/M and

M phase populations, respectively, of MCF7 cells. However, the double thymidine block approach with nocodazole or nocodazole-coupled mitotic shake-off is more effective in enriching S, G2/M, or M phase populations of T47D cells.

Keywords: Breast Cancer, Cell Cycle, Estrogen, Estrogen Receptor, Synchronization

ÖZ

MEME ADENOKARSİNOMLARINDAN ELDE EDİLEN SENKRONİZE ÖSTROJEN RESEPTÖRÜ POZİTİF HÜCRE MODELLERİNİN HÜCRE DÖNGÜSÜ FAZLARININ ZENGİNLEŞTİRİLMESİ

Toker, Pelin
Yüksek Lisans, Moleküler Biyoloji ve Genetik
Tez Yöneticisi: Prof. Dr. Mesut Muyan

Ağustos 2024, 69 sayfa

17β-östradiyol (E2), dolaşımdaki ana östrojen hormonu olarak meme dokusunun büyümesi, farklılaşması ve işlevi için kritik bir sinyal faktörüdür. E2'nin meme dokusu üzerindeki etkileri başlıca östrojen reseptörü α (ERα) aracılığıyla sağlanır ve E2-ERα sinyalindeki düzensizlikler meme kanserinin başlamasına/ilerlemesine ve tedavilere karşı dirence katkıda bulunur. Meme kanseri hücre hatları in vitro model sistemleri olarak, hücresel olaylar, ilaç keşfi ve ilaç direnci konusunda paha biçilemez içgörüler sağlar. ERα sentezleyen hücre hatları arasında, MCF7 ve T47D hücreleri, E2-ERα tarafından aracılık edilen hücresel çoğalmayı koordine eden hücre döngüsü fazlarına özgü moleküler olayları açıklamak için yaygın olarak kullanılır. Hücre döngüsü fazlarında zenginleştirilmiş popülasyonlar oluşturmak için kullandığımız çeşitli yaklaşımlarla elde ettiğimiz değişken sonuçlar nedeniyle, MCF7 ve T47D hücrelerinde, etkili bir hormon çekilim yaklaşımı olan kömür dekstranla muamele edilmiş fetal sığır serumu, yani CD-FBS'yi tek başına veya DNA replikasyon inhibitörü olan fazla timidin ve/veya mikrotübül zehri olan nokodazol ile birlikte kullanarak hücre döngüsü senkronizasyonuna bağlı faz zenginleştirmesini yeniden değerlendirmek istedik. Hormon çekiliminin hem MCF7

hem de T47D hücrelerini G0/G1 fazında senkronize ettiğini bulguladık. CD-FBS'ye E2 ilave edilmesi S faz popülasyonunu zenginleştirmekte; nokodazol ve nokodazol ile birleştirilmiş mitotik silkeleme ise MCF7 hücrelerinin sırasıyla G2/M ve M faz popülasyonlarını artırmaktadır. Ancak, çift timidin bloğu yaklaşımıyla birlikte nokodazol veya nokodazol ile birleştirilmiş mitotik silkeleme, T47D hücrelerinin S, G2/M veya M faz popülasyonlarını zenginleştirmede daha etkilidir.

Anahtar Kelimeler: Meme Kanseri, Hücre Döngüsü, Östrojen, Östrojen Reseptörü, Senkronizasyon

To those who may feel lost while searching for their own path

ACKNOWLEDGMENTS

First and foremost, I would like to thank my supervisor Prof. Dr. Mesut Muyan for guiding me in my journey into the scientific world with endless patience and support. His mentorship has been invaluable in shaping me into a better scientist.

I would like to thank my thesis committee members, Prof. Dr. Ayşe Elif Erson Bensan and Assist. Prof. Dr. Bahar Değirmenci Uzun, for their time and feedback.

I want to express my heartfelt thanks to all the members of Muyan Lab for both their experimental help and moral support. I cannot give enough thanks to Hazal Ayten, who is not only my lab buddy, but also my best friend and partner in crime. I find myself extremely lucky that our paths crossed because she brought light and color to my life. Special thanks to Annageldi Ashyralyyev, for his kind heart and for being a brilliant lab mate. I extend my appreciation to Dr. Pelin Yaşar, Dr. Begüm Akman and Gizem Güpür for their valuable mentorship; and to Gizem Turan Duman, Çağla Ece Olgun and Büşra Bınarcı, as well as our previous members Öykü Demiralay, Kerim Yavuz and Gizem Kars for all their teachings and support.

I am grateful to the members of Erson Lab, especially İrem Yılmazbilek, Elanur Almeriç, and İrem Eroğlu for our cheerful conversations. To my dearest friends, Atakan Turan, Hakan Sönmez, and Gürkan Kısaoğlu, your unwavering support and friendship has been invaluable through this journey.

Last but not least, I want to thank my family for their endless love and patience. I am thankful to my dad and my older brother for always believing in me and supporting my decisions. However, I could not have reached where I am today without my mom’s efforts and sacrifices, for which I am deeply grateful.

I would like to thank TÜBİTAK for supporting me through the National MSc Scholarship Program, and for supporting this study under the grant numbers 121Z346 and 114Z243.

TABLE OF CONTENTS

LIST OF TABLES

TABLES

LIST OF FIGURES

FIGURES

LIST OF ABBREVIATIONS

ABBREVIATIONS

ER: Estrogen receptor

E2: 17β-estradiol

ERE: Estrogen-responsive element

CDK: Cyclin-dependent kinase

DTB: Double thymidine block

CD: Dextran-coated charcoal

EtOH: Ethanol

4-HTam: 4-hydroxytamoxifen

ICI: Imperial Chemical Industries 182,780

Aph: Aphidicolin

Noc: Nocodazole

PI: Propidium iodide

RDTB: Release from DTB

CHAPTER 1

INTRODUCTION

1.1 Breast Cancer

Breast cancer is the second most common cancer type in the world when both sexes are taken into account, and it is the most common cancer type in women worldwide as well as the deadliest[1]. It is estimated that in 2024, 310,720 women will be diagnosed with invasive breast cancer, and 42,250 women will die due to breast cancer in USA[2]. In Türkiye, breast cancer ranks first among the ten most common cancer types that cause death in women, with approximately 24,000 new cases seen annually and approximately 5% of these cases resulting in mortality, the rate of which is higher than in the USA[3,4]. As breast cancer is such a threatening disease, especially for females, it has been crucial to elucidate the underlying mechanisms for the development of diagnostic and/or treatment tools.

The heterogeneity of breast cancer is one of the reasons for its fatality since it contributes not only to the progression of the cancer, through proliferation and metastasis but also resistance to treatment[5]. Prior to the development of molecular screening techniques, the classification of breast cancer was based on histopathological observations regarding the histological type, histological grade, tumor size, and lymph node status, as well as immunohistochemical assessment of biomarkers such as estrogen receptor (ER), progesterone receptor (PR), and human epidermal growth factor receptor 2 (HER2)[6,7]. Nowadays, with the use of gene expression profiling, breast cancers can be classified based on their genomic and transcriptomic features[6]. This molecular classification also enabled the identification of further subtypes; nevertheless, breast cancers can be mainly classified as:

1) Luminal A (ER^+, $PR^{+/-}$, $HER2^-$),

2) Luminal B (ER^+, $PR^{+/-}$, $HER2^+$),
3) Triple-negative (ER^-, PR^-, $HER2^-$),
4) HER2 positive (ER^-, PR^-, $HER2^+$) [7].

Among these subtypes, luminal A type breast cancer is the most prevalent one, corresponding to about 50-60% of the patients[8]. Although patients with luminal A type cancer have been reported to have a good prognosis[8], the high prevalence rate of this subtype renders both the past and future research valuable.

For breast cancer research, established cell lines have been highly essential in vitro models that provide information with potential highly beneficial in the clinic[7]. Specifically, MCF7 and T47D cell lines are widely used models that are derived from the luminal A subtype of breast cancer[7]. The MCF7 cell line was established from the pleural effusion taken from a 69-year-old Caucasian female patient with metastatic breast carcinoma[9]. Likewise, the T47D cell line was derived from the pleural effusion of a 54-year-old female patient with infiltrating ductal carcinoma[10]. Despite having distinct molecular characteristics, both MCF7 and T47D cell lines have been used for understanding the mechanisms of estrogen-estrogen receptor (ER) α signaling, as well as the cellular events mediated in response to this signaling pathway since they are estrogen-responsive and ERα-synthesizing breast cancer models[11–14]. Thus, these cell lines have been significant experimental models in studies regarding estrogen-ERα signaling that we have been conducting in our laboratory as well.

1.2 Estrogen Signaling

Estrogen signaling is a critical pathway for breast cancer as overexpression of estrogen receptors is observed in around 70% of invasive breast carcinomas[15]. This pathway, through estrogen receptors, regulates genes that are involved in cell proliferation, differentiation, and migration; hence, deregulation of estrogen

signaling in the breast tissue contributes to the initiation and/or progression of breast cancer[15,16].

17β-estradiol (E2) has significant roles in the regulation of physiology and pathophysiology of different tissues, including breast tissue, as the main circulating estrogen hormone[17]. This regulatory effect of E2 is mediated by estrogen receptor (ER) α and β, which are transcription factors, and they are expressed in the same tissue or different tissues in varying levels[17]. Even though ERα and ERβ are encoded by two distinct genes, *ESR1* and *ESR2* respectively, they have similar structural and functional features[17,18].

The ERs consist of six functional domains that are named from A to F starting from the amino terminus of the receptors, as represented in Figure 1. The A/B domain has a ligand-independent transactivation function AF-1, whereas the other activation function comes from the ligand-dependent transactivation function AF2 in the E/F domain located in the carboxyl-terminus. The E/F domain is also involved in ligand binding as well as dimerization. The highest conserved domain between ERs is the C domain, which is the DNA-binding domain (DBD). Lastly, the D domain, as the flexible hinge, not only links the C and E/F domains, but also contains a nuclear localization signal[19].

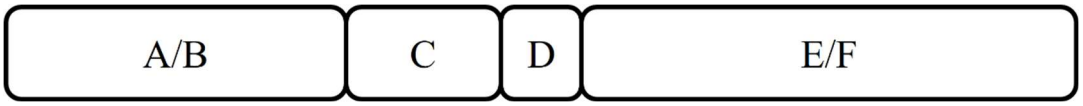

Figure 1. Schematic representation of domains of estrogen receptors.

After it is synthesized, ERα dimerizes and, while a small fraction of the newly synthesized ERα moves to the peri-membrane, cytoplasm, or mitochondria, translocates to the nucleus even without E2. On the other hand, when E2 binds to ERα, the ligand binding domain of ERα undergoes a conformational change that allows protein-protein interactions, hence rendering ERα functionally active[20]. The E2-ERα complex in its active form then mediates genomic events that lead to the

regulation of target gene expressions either through estrogen-responsive element (ERE)-dependent or ERE-independent pathways. In the ERE-dependent pathway, the E2-ERα complex interacts with EREs on DNA, which are palindromic sequences with the consensus sequence of 5′-GGTCAnnnTGACC-3′[20]. Although the unliganded ERα inefficiently interacts with EREs, binding of E2 to ERα is critical for ERE-dependent signaling as it increases the stability of E2-ERα-ERE interactions[21]. In contrast, instead of directly interacting with its response elements on DNA, the E2-ERα complex can interact with transcription factors that are bound to their cognate regulatory elements on DNA, such as AP1 (activator protein 1), and SP1 (stimulatory protein 1), which also results in the regulation of transcription of E2-ERα target genes. This pathway is known as the ERE-independent pathway[17,20].

Consequently, both ERE-dependent and independent pathways lead to the regulation of responsive genes involved in cell proliferation, differentiation, motility, and death[20], and the altered expression of these target genes is a contributor to the initiation and/or the progression of breast cancer[16]. Thus, elucidating the sequence of events that coordinate cellular proliferation in response to the E2-ERα signaling carries significance for the development of effective prognostic and therapeutic tools. This necessitates the identification of factors and the delineation of their functions in the initiation and progression of cell cycle phases that culminate in cell division.

1.3 Cell Cycle

The cell cycle is a strongly regulated series of events that results in the replication and distribution of the genetic material to the daughter cells by cell division[22]. The cell cycle consists of four phases: G1 (gap 1), S, G2 (gap 2), and M (mitosis). In the G1 phase, certain mitogens and growth factors stimulate the cell for preparation for DNA synthesis and subsequent cell division. The phase where DNA replication occurs is known as the S phase, and after completing the DNA replication successfully, the cell progresses to the second gap in the cycle, which is the G2 phase.

Following G2, the cell goes through the M phase, i.e. mitosis, which involves the segregation of the duplicated DNA and is completed by cell division[22,23]. Additionally, the cells that have temporarily or permanently withdrawn from the cell cycle are defined to be quiescent, or in the G0 phase. These cells can exit G0 and re-enter the cell cycle from G1 in response to the external stimulants[22].

To ensure an orderly progression of the cells through each phase, there are certain checkpoints the cells need to go through for commitment to the next phase. The first one takes place in the late G1, also known as the restriction point; the second one takes place in the late G2, before entering mitosis; and the last one is in the M phase, which is also known as the spindle checkpoint, and is critical for the correct distribution of duplicated DNA and exit from mitosis[24,25]. The progression through these checkpoints as well as the cell cycle phases are regulated by cyclin-dependent kinases (CDKs) which act together with cyclins[23].

One primary event involved in the initiation/development of cancer involves disruptions in the normal cell cycle. Understanding how the cell cycle is regulated and how it becomes dysregulated in disease states provides valuable insights into the underlying mechanisms critical for the disease. This in turn provides opportunities for the identification of drug targets, drug screening, and/or effective drug selection or development.

Cell cycle synchronization by various approaches therefore provides unique opportunities for a better understanding of molecular events critical for the regulation and progression of the cell cycle phases.

1.3.1 Approaches for cell cycle synchronization

Approaches for cell cycle synchronization are centered around physical fractionations and chemical/pharmacological agents with varying advantages and disadvantages. Physical fractionation techniques are based on the size and density of cells by centrifugal separation as well as light scatter or fluorescent emission of

labeled cells using a flow cytometer or fluorescence-activated cell sorter. Because of nonuniform size distributions of tumorigenic cells due to polyploidy, low cellular yields, and dependency on specialized equipment in physical fractionation techniques, chemical/pharmacological agents that primarily target DNA synthesis or mitotic spindle formation for the transient inhibition of cell cycle phase transitions have been widely used for synchronization studies[26–28].

Based on the interruption of the deoxynucleotide metabolism pathway through competitive inhibition with excess thymidine, double thymidine block (DTB) is one of the most frequently used chemical methods that has been used to arrest cells at the G1/S boundary before DNA replication[27,29]. Aphidicolin is another widely used chemical agent that arrests the cells at the G1/S transition by reversibly inhibiting the functions of DNA polymerase α, which in turn prevents DNA replication in S phase[30]. On the other hand, nocodazole and colchicine are popular chemical agents for G2/M arrest, which is mediated by the inhibition of mitotic spindle formation[27]. G2/M arrest is often coupled with a mitotic shake-off that yields a highly enriched mitotic cell population[28].

As estrogen has mitogenic effects on estrogen-responsive ER-positive breast cancer cell lines, withdrawal of estrogen from cell culture environments that primarily rely on dextran-coated charcoal (CD) treatment of fetal bovine serum (FBS), CD-FBS, has been used as an effective mean for cell cycle synchronization of cell models derived from breast adenocarcinomas[31–33]. Subsequent supplementation of synchronized cells with estrogen alone or together with chemical/pharmacological agents has provided experimental systems for specific cell cycle phase enrichments.

1.4 Aim of This Study

Among the various approaches utilized for cell cycle synchronization, we employed certain chemical/pharmacological agents, alone or in combinations, to enrich cell cycle phases in breast adenocarcinoma-derived E2-responsive and ERα-synthesizing

MCF7 and T47D cells in our laboratory. However, we obtained results with reproducibility and reliability issues that limited the utility of some of these approaches. We have also utilized E2 withdrawal using CD-FBS, and subsequent treatment of the cells with E2 alone or in combination with different chemical/pharmacological agents. Nevertheless, various factors including the preparation and use of CD-FBS, as well as the nature, concentration, and duration of chemical/pharmacological agents in cycle synchronizations can also generate experimental variability undermining reproducibility[32,34].

In this study, we aimed to reassess cell cycle synchronization-based phase enrichment approaches with CD-FBS alone or in combination with chemical/pharmacological agents in MCF7 and T47D cells to provide a standardizable framework for cell cycle studies. We also used, without or with CD-FBS, the DTB approach as a widely utilized chemical cell cycle synchronization method for G1/S arrest for comparative analysis.

CHAPTER 2

MATERIALS AND METHODS

2.1 Cell Lines, Growth Conditions and Cell Cycle Synchronization

2.1.1 Cell growth

The MCF7 cell line obtained from ATCC (https://www.atcc.org/) was a kind gift from Prof. Dr. Özgür Şahin (Bilkent University, Turkey), and the T47D cell line from ATCC (https://www.atcc.org/) was a kind gift from KanSiL (Middle East Technical University, Türkiye). MCF7 cells were maintained in high glucose (4.5g/L) containing Dulbecco's modified eagle medium (DMEM, Sartorius, Israel, 01-053-1A) without phenol red, supplemented with 10% fetal bovine serum (FBS, Sartorius, 04-007-1A), 1% penicillin-streptomycin (Sartorius, 03-031-1B), and 1.2% L-glutamine (Sartorius, 03-020-1B). T47D cells were grown in Roswell Park Memorial Institute 1640 medium (RPMI 1640, Sartorius, 01-103-1A) without phenol red, supplemented with 10% FBS, 1% penicillin-streptomycin, and 1.2% L-glutamine.

Both MCF7 and T47D cells were maintained in up to eight passages in a humidified incubator with 5% CO_2 at 37°C. The corresponding medium of cell lines was refreshed every three days.

2.1.2 Preparation of CD-treated FBS (CD-FBS) and efficiency control

For an efficient removal of E2 from the FBS, charcoal dextran (CD) treatment of FBS has been utilized in our laboratory. 10 g of CD (Sigma Aldrich, USA, C6241) was added to a 500 ml FBS bottle. FBS with the added CD was stirred slowly, to

prevent breaking CD into smaller particles, with an autoclaved magnetic stirrer bar on a magnetic stirrer for 16 hours at 4°C. Then the CD-FBS mixture was divided into two Nalgene PPCO centrifuge bottles (Thermo Fisher Scientific, USA, 3120-9500) in equal volumes and centrifuged at 10,800 x g for 30 minutes at 4°C using Sorvall SLA-3000 rotor. The supernatant from the two bottles was decanted, without disturbing the pellet, into a low protein binding, 500 ml sterile filter unit with 0.45 µm pore size (Corning, USA, 430770) and filtered inside the laminar flow cabinet. Another 10 g CD was added to the filtrate for the second round of CD treatment. The mixture was stirred on the magnetic stirrer in the same manner as described above, for 4 hours at 4°C. The CD-treated FBS was divided into two Nalgene PPCO centrifuge bottles in equal volumes and centrifuged at 10,800 x g for 30 minutes at 4°C using Sorvall SLA-3000 rotor once more. The supernatant from the bottles was combined and filtered using the 500 ml sterile filter unit with 0.45 µm pore size first, then filtered through a low protein binding, 500 ml sterile filter unit with 0.22 µm pore size (Corning, 431097) for the second time inside the laminar flow cabinet. The filtrate, CD-FBS, was then aliquoted into 50 ml falcon tubes and stored at -20°C.

Both MCF7 and T47D cells were used to test the newly prepared CD-FBS. MCF7 cells (2 x 10^5 cells/well) or T47D cells (2.5 x 10^5 cells/well) were plated to 6-well tissue culture plates in their respective growth media, DMEM or RPMI 1640 supplemented with 10% FBS, 1% penicillin-streptomycin, and 1.2% L-glutamine, and grown for 48 hours. At the end of 48 hours, cells were washed twice with 1x Phosphate Buffer Saline (PBS, Sartorius, 02-023-5A), and refreshed with their respective growth media supplemented with 10% CD-FBS, 1% penicillin-streptomycin, and 1.2% L-glutamine. The cells were incubated in CD-FBS containing growth media for 72 hours, and the media were refreshed at 48 hours. Following the 72-hour incubation, a portion of the cells were collected with trypsinization (0h), whereas the remainder were treated with 10^{-9} M 17β-estradiol (E2, Sigma Aldrich, E2257), which is the upper physiological level of circulating hormone in adult women [35] (also Supplementary Data, Figure 12), or with 0.01% ethanol (EtOH, Sigma Aldrich, 1.00983) as vehicle control for 24 hours. After 24

hours, cells were collected with trypsinization to assess cell cycle profiles with flow cytometry (which is described in further detail in section 2.2), and *TFF1/pS2* expression (which is explained further in section 2.4). It was confirmed that E2 was effectively removed from FBS with CD treatment if 1) the cells were accumulated at the G1 phase at the end of 72-hour CD-FBS incubation, 2) E2 triggered cell cycle progression when compared to ethanol control, and 3) *TFF1/pS2* expression was increased in E2 treated cells in comparison to ethanol given cells (Supplementary Data, Figure 13).

2.1.3 Synchronization of cell cycles with E2 withdrawal

To synchronize the cell cycles of MCF7 and T47D cells using CD-FBS containing growth media, MCF7 (7.5×10^5 cells/flask) or T47D (10×10^5 cells/flask) cells were plated in T-25 tissue culture flasks in the DMEM or RPMI 1640 medium, respectively, supplemented with 10% CD-FBS and incubated for 72 hours with media change at 48 hours. After this 72-hour incubation, cells were treated with either 10^{-9} M E2 or 0.01% EtOH for a total of 36 hours with 3- to 6-hour intervals in their respective growth media supplemented with 10% CD-FBS. At each time point, cells were collected with trypsinization, and a portion of the cells was used for flow cytometry, whereas the other portion was used for protein isolation and subsequent Western Blot (WB) analyses, which is further described in section 2.3. To prepare the cells for either process, the collected cells were pelleted, washed with 1x PBS, and then pelleted again. For flow cytometry, the pelleted cells were resuspended in 100 µl of 1x PBS containing 2% CD-FBS and fixed with a dropwise addition of ice-cold 70% ethanol. The fixed cells were stored at -20°C overnight before flow cytometry reading. For protein isolation, the cell pellet was processed freshly as described in section 2.3.

2.1.4 Treatment of cells with 4-hydroxytamoxifen (4-HTam) or Imperial Chemical Industries 182,780 (ICI)

To test if cell cycle progression of MCF7 or T47D cells is dependent on E2-ERα signaling, 4-HTam (Sigma Aldrich, H7904), a selective estrogen receptor modulator[36], or ICI (Tocris Bioscience, UK, 1047), a selective estrogen receptor down-regulator[37], were utilized. For the selection of the optimal dose for both 4-HTam and ICI, MCF7 cells were plated and grown in DMEM supplemented with 10% FBS. Then the cells were treated with varying doses of 4-HTam or ICI, ranging from 10^{-10} to 10^{-6} M, for 24 hours. Following the treatment, the cells were collected by trypsinization for flow cytometry analyses (Supplementary Data, Figure 14A & 14C).

For the synchronization of MCF7 cells using 4-HTam, the cells plated and grown in DMEM supplemented with 10% FBS were treated with 10^{-7} M 4-HTam or its vehicle control 0.0002% DMSO for 48 hours. Similarly, for synchronization of MCF7 cells using ICI, the cells plated and grown in their normal growth medium were treated with 10^{-7} M ICI, or its vehicle control 0.01% ethanol for 48 hours. Following the 48-hour treatment, a portion of the cells (0h) were collected and either fixed and subjected to flow cytometry analysis or processed for protein isolation and Western Blot analysis. The remaining cells were washed with 1x PBS twice and their media were refreshed with the normal growth medium for 72 hours. The cells were then collected for flow cytometry and Western Blot analyses at 24-hour intervals.

Moreover, MCF7 or T47D cells, which were synchronized at G0/G1 with 72-hour CD-FBS incubation, were then treated without (vehicle) or with 10^{-9} M E2 and/or 10^{-7} M 4-HTam or ICI for 24 hours to test the dependency of cell cycle progression on E2-ERα signaling. At the end of treatments, the cells were collected, and a portion of cells were fixed and subjected to flow cytometry analysis, whereas the remaining part was processed for protein isolation and Western Blot analysis (Supplementary Data, Figure 14B & 14D).

2.1.5 Synchronization of cell cycles with the double thymidine block (DTB) approach

For the synchronization of cell cycles with double thymidine block, MCF7 (5 x 10^5 cells/flask) or T47D (7.5 x 10^5 cells/flask) cells were plated and grown in T-25 tissue culture flasks for 72 hours. The cells were then incubated in growth media containing 10% FBS and 2 mM thymidine, which was based on a concentration that was maximally effective in cell synchronization at the G1/S boundary without inducing toxicity[29], for 14 hours (Supplementary Data, Figure 15). The cells were released from thymidine treatment by washing the cells twice with 1x PBS and re-incubating them with normal growth media containing 10% FBS without thymidine for 12 hours. After 12 hours, the media of the cells were changed with media containing 10% FBS and 2 mM thymidine and the cells were incubated for 22 hours. Cells were re-released from thymidine treatment by washing the cells twice with 1x PBS and maintaining them in the respective growth media containing 10% FBS. Cells were collected with trypsinization at different time points for flow cytometry and Western Blot analyses up to 16 hours.

To assess the effects of E2 on the DTB approach, MCF7 (7.5 x 10^5 cells/flask) or T47D (10 x 10^5 cells/flask) cells were plated and grown in T-25 tissue culture flasks in media supplemented with 10% FBS for 72 hours. The cells were then washed twice with 1x PBS, and they were incubated in media containing 10% CD-FBS and 2 mM thymidine for 14 hours. The cells were then released from thymidine treatment by washing cells twice with 1x PBS and incubating them in 10% CD-FBS containing appropriate media for 12 hours. Then, the media of the cells were changed with media containing 10% CD-FBS and 2 mM thymidine and the cells were incubated for an additional 22 hours. Cells were subsequently incubated in media containing 10% CD-FBS without (0.01% EtOH as the vehicle control for E2) or with 10^{-9} M E2 for various intervals up to 32 hours. Cells were collected with trypsinization at different time points for flow cytometry and Western Blot analyses.

2.1.6 Treatment of cells with aphidicolin, 2,3-DCPE, or nocodazole

For enrichment of S, G2, and/or M phases in MCF7 or T47D cells, various chemical agents such as aphidicolin (Tocris Bioscience, 5736), 2,3-DCPE (Tocris Bioscience, 2137) or nocodazole (Sigma-Aldrich, 487928) were utilized. Aphidicolin is a DNA polymerase inhibitor that arrests cell cycle progression at the G1/S transition[30]. To enrich the S phase population, the cells were either treated with 10 μM of aphidicolin, which is based on previous studies of dose optimization[38], or with DMSO as the vehicle control for 6 hours in the presence of E2 following different durations of E2 treatment of cells synchronized at G0/G1. The cells were then collected by trypsinization for flow cytometry analysis. Likewise, 2,3-DCPE is a compound that induces S phase arrest[39]. The cells synchronized at G0/G1 were initially incubated with E2 for 6 hours and then treated with 20 μM 2,3-DCPE[38] or with 1x PBS as the vehicle control for 12 hours in the presence of E2. Following treatment, the cells were collected by trypsinization for flow cytometry analysis.

Nocodazole, on the other hand, is an anti-mitotic agent that arrests the cells in G2/M phases[27]. To select the optimal dose of nocodazole, MCF7 cells were first synchronized at the G0/G1 phase by 72-hour CD-FBS incubation, then treated with 10^{-9} M E2 for 21 hours. Following incubation with E2, the cells were treated with 0.3, 0.6, or 1.2 μM nocodazole, or with DMSO as the vehicle control for 6 hours in the presence of E2. The cells were then subjected to mitotic shake-off by tapping the flasks to collect the mitotic cells, and the remaining attached cells were collected by trypsinization for flow cytometry analysis. After deciding that 0.3 μM was the optimal dose for nocodazole treatment, the cells synchronized at the G0/G1 phase were treated with E2 for various durations (18, 21, 24 hours), and then supplemented with 0.3 μM nocodazole or DMSO for 6 hours in the presence of E2 to select the optimal time point to start the nocodazole treatment. The cells were subjected to mitotic shake-off and the remaining cells were trypsinized to assess the cell cycle phase distributions using flow cytometry.

2.2 Flow Cytometry

For the assessment of cell cycle distributions using flow cytometry, 1 x 10^6 cells were taken into a 15 ml falcon and centrifuged at 300 x g for 6 minutes to remove the trypsin and medium. The supernatant was aspirated, and the cell pellet was washed with 500 µl 1x PBS. The cells were centrifuged again at 300 x g for 7 minutes and the supernatant was aspirated again. The cell pellet was resuspended in 100 µl of 1x PBS containing 2% CD-FBS and fixed with a dropwise addition of 4 ml ice-cold 70% ethanol while being gently vortexed to prevent clumping. The fixed cells were stored at -20°C overnight, or up to 1 week maximum, before flow cytometry reading.

To prepare the cells for flow cytometry reading, the cells were centrifuged at 300 x g for 7 minutes to remove the 70% ethanol. After ethanol was aspirated, the pellet was washed with 500 µl ice-cold 1x PBS, and the cells were centrifuged again at 600 x g for 7 minutes. Then the supernatant was aspirated again, and the cell pellet was resuspended in 200 µl 1x PBS containing 20 µg/ml propidium iodide (PI, Sigma Aldrich, P4170), 200 µg/ml RNase A (Thermo Fisher Scientific, EN0531), and 0.4% (v/v) Triton X-100 (AppliChem, Germany, A4975). The cells were then incubated for 30 minutes in the dark at room temperature. Following incubation, the cells were analyzed with a NovoCyte Flow Cytometer (Agilent Technologies, USA) using the PI channel. A sample gating strategy is given in Appendix D.

2.3 Total Protein Isolation and Western Blot

For total protein isolation, the collected cells were pelleted once, washed with 1x PBS, and pelleted again. The cell pellets were then resuspended with RIPA buffer (Appendix E) containing freshly added 1x protease inhibitor (Roche, Switzerland, 11697498001) and 1x phosphatase inhibitor (Roche, 4906845001), and incubated on ice for 30 minutes. The cells were actively sonicated for 1 minute (6 cycles of 10-second sonication, 15-second pause), and centrifuged at 16,000 x g for 20 minutes.

The supernatants were collected, and protein concentrations were assessed with Quick Start Bradford Protein Assay (Bio-Rad, USA, 500-0201).

For Western Blot analysis, 6x Laemmli buffer (Appendix E) was added to the protein extracts, and the protein samples were incubated at 95°C for 10 minutes for denaturation. The protein samples were separated on 10% SDS-PAGE at 100 V for 90 minutes and then transferred to a PVDF (polyvinylidene difluoride) membrane (Roche, 03010040001) using wet-transfer at 100 V for 70 minutes. Additionally, for the WB analysis of the Ki-67 protein, protein extracts were subjected to 4-20% SDS-PAGE, and the wet-transfer was performed at 100 V for 120 minutes. Following the transfer, the membranes were blocked with 5% skim milk (Merck, 70166) in 0.1% TBS-T (Tris Buffered Saline- Tween) at room temperature for 1 hour. Membranes were then incubated at room temperature for 1 hour with the primary antibody specific for Cyclin B1 (Santa Cruz Biotechnology, USA, sc-245) in 1:500, Cyclin E (Santa Cruz Biotechnology, sc-247) in 1:250, Ki-67 (Thermo Fisher Scientific, RM-9106-S0) in 1:500, or HDAC1 (Santa Cruz Biotechnology, sc-81598) in 1:1000 dilution in 0.1% TBS-T containing 5% skim milk; or ERα (Santa Cruz Biotechnology, sc-543) in 1:1000 dilution in 0.05% TBS-T containing 5% skim milk. A horse radish peroxide (HRP) conjugated goat anti-mouse secondary antibody (Advansta, USA, R-05071) was used in 1:5000 dilution in 0.1% TBS-T containing 5% skim milk for Cyclin B1, Cyclin E, Ki-67 and HDAC1 antibodies. Similarly, HRP conjugated goat anti-rabbit secondary antibody (Advansta, R-05072) was used in the same dilution for the ERα antibody. The membranes were incubated with the secondary antibody at room temperature for 1 hour. The protein bands were visualized with WesternBright enhanced chemiluminescence (ECL) kit (Advansta, K-12045) using the ChemiDoc^{TM} MP system (Bio-Rad), and Image Lab 6.1 software was used for the analyses of the generated images.

2.4 Expression Analysis

MIQE Guidelines[40] were followed in total RNA isolation, cDNA synthesis, and RT-qPCR steps, and the MIQE checklist is presented in Appendix C.

2.4.1 Total RNA isolation

For each experimental group, the cells were collected with trypsinization, and 30 x 10^4 cells were separated for total RNA isolation. These cells were washed twice with 1x PBS and pelleted. The pellets were stored at -80°C until RNA isolation. Total RNA isolation was performed using a NucleoSpin RNA Kit (Macherey-Nagel, Germany, 740955.50), which also includes an on-column DNase treatment step, according to the manufacturer's instructions. Following RNA isolation, the samples were subjected to the RNA clean-up protocol with a second on-column DNase treatment for effective removal of genomic DNA. The concentrations of the RNA samples were measured with Nanodrop 2000 (Thermo Fisher Scientific), as well as the A260/A280 and A260/A230 ratios for the assessment of purity of the samples.

2.4.2 Genomic DNA contamination control in RNA samples

To ensure that the RNA samples were free of genomic DNA contamination, 300 ng of RNA from each sample was used as a template in a PCR reaction using primers specific to glyceraldehyde-3-phosphate dehydrogenase (*GAPDH*). The primer sequences are as follows: GAPDH_FP: 5'-GGGAGCCAAAAGGGTCATCA-3' and GAPDH_REP: 5'-TTTCTAGACGGCAGGTCAGGT-3. The PCR was performed using Taq DNA polymerase (Thermo Fisher Scientific, EP0401) with the cycling conditions given in Table 1. 50 ng of MCF7 genomic DNA was used as positive control. After the PCR was completed, the PCR products were run on 2% (w/v) agarose gel for visualization. If the RNA samples did not contain genomic DNA, they were used in cDNA synthesis. In the case of genomic DNA

contamination, the RNA samples were re-subjected to the RNA clean-up protocol with an on-column DNase treatment until they were free of genomic DNA.

Table 1. PCR cycling conditions for *GAPDH*

Step	Temperature (°C)	Duration	Number of cycles
Initial denaturation	95	3 min	1
Denaturation	95	30 sec	40
Annealing	65	30 sec	
Extension	72	30 sec	
Final extension	72	10 min	1
Hold	4	∞	1

2.4.3 cDNA synthesis

For cDNA synthesis from the total RNA samples, the RevertAid First Strand cDNA Synthesis Kit (Thermo Fisher Scientific, K1622) was used. 300 ng of RNA was used as the template with oligo $(dT)_{18}$ primers in the reactions per the manufacturer's instructions. The reaction components and their respective amounts/volumes are specified in Table 2. The cDNA synthesis was carried out at 42°C for 1 hour using T100 Thermal Cycler (Bio-Rad), and the reaction was terminated by incubation at 70°C for 5 minutes. The cDNA samples were kept at -80°C for long-term storage.

Table 2. Reaction components for cDNA synthesis

Component	Amount
Total RNA	300 ng
Oligo $(dT)_{18}$ Primer	1 µl
5x Reaction Buffer	4 µl
10 mM dNTP Mix	2 µl
RiboLock RNase Inhibitor (20 U/µl)	1 µl
RevertAid M-MuLV RT (200 U/µL)	1 µl
Nuclease-free Water	Up to 20 µl

2.4.4 *TFF1/pS2* expression analysis with RT-qPCR

Trefoil factor 1 (*TFF1/pS2*) is a well-characterized E2-ERα responsive gene[19,41], hence its expression has been used as a control for E2 response in our laboratory. To assess the *TFF1/pS2* expression, RT-qPCR was performed using a Rotor-Gene Q (Qiagen, Germany) PCR machine with primers specific to *TFF1*. The primer sequences are as follows: pS2/TFF1_FP: 5'-TTGTGGTTTTCCTGGTGTCA-3' and pS2/TFF1_REP: 5'- CCGAGCTCTGGGACTAATCA-3' (product size: 209 bp). 300 nM of each primer as well as the SsoAdvanced Universal SYBR Green Supermix (Bio-Rad, 1725272) and 2 µl of 1:20 diluted cDNA template were used in each 10 µl RT-qPCR mix with the cycling conditions given in Table 3.

Table 3. RT-qPCR cycling conditions for *TFF1/pS2*

Step	Temperature (°C)	Duration	Number of cycles
Initial denaturation	94	10 min	1
Denaturation	94	30 sec	40
Annealing	55	30 sec	
Extension	72	30 sec	
Melting	55-99	-	1

Ribosomal protein lateral stalk subunit P0 (*RPLP0*) was reported as a consistent reference gene for normalization in RT-qPCR analysis for breast carcinomas[42]. Therefore, *RPLP0* was used for normalization in the expression analysis of *TFF1*. The sequences of the primers specific to *RPLP0*, that were used in the RT-qPCR, are as follows: RPLP0_FP: 5'-GGAGAAACTGCTGCCTCATA-3' and RPLP0_REP: 5'-GGAAAAAGGAGGTCTTCTCG-3' (product size: 191 bp). The RT-qPCR was performed with the following cycling conditions: Initial denaturation at 94°C for 10 minutes; 40 cycles of denaturation at 94°C for 30 seconds, annealing at 60°C for 30 seconds, and extension at 72°C for 30 seconds.

For the expression analysis, three biological replicates were used, and the RT-qPCRs for both *TFF1* and *RPLP0* were performed with three technical replicates for each biological replicate. To quantify the relative expression of *TFF1*, $\Delta\Delta C_t$ calculation was utilized[43], and while calculating the fold change, the expression level of ethanol-treated samples was set to 1 and the expression levels of E2-treated samples were calculated in comparison to ethanol groups. One-tailed paired t-test with a 95% confidence interval was used for the statistical analysis, and the analysis and visualization were performed using GraphPad Prism 8.0.2 (GraphPad Software, USA).

CHAPTER 3

RESULTS AND DISCUSSION

3.1 Synchronization of the Cell Cycle of MCF7 Cells with CD-FBS with or without E2 Replacement

FBS is a growth supplement for cell and tissue culture media required for attachment, growth, proliferation, and differentiation of human and animal cells[34]. It contains various peptide and steroid hormones, growth factors, amino acids, proteins, vitamins, inorganic salts, carbohydrates, and antibodies as well as potential adverse factors including endotoxin, mycoplasma, and/or viral contaminants[34,44,45]. The treatment of FBS with charcoal dextran removes a variety of non-polar/lipophilic components, including steroid hormones[32,46]; hence, the use of CD-treated FBS (CD-FBS) in culture media allows the examination of the effects of these components on cellular events in culture systems[47]. However, there might be some content variations in FBS that arise from the diversity of geographical and seasonal sources as well as from varying approaches used institutionally or commercially for the CD treatment of FBS[32,34]. These variations in FBS content may in turn affect the extent of serum component deprivation, thereby generating experimental variability and reproducibility issues[32], as it has been encountered in our laboratory on several occasions. Therefore, we employed a laboratory-optimized condition for the treatment of FBS twice with CD as described in section 2.1.2, and used it in cell cycle synchronization studies.

To assess the effects of estrogen withdrawal on cell cycle progression, MCF7 cells were synchronized by maintaining them in DMEM containing 10% CD-FBS for 72 hours. Under this condition, more than 80% of the cell population accumulated at the G0/G1 phase as assessed by flow cytometry (Figure 2A). To examine the effects of E2 on cell cycle phase transitions, cells arrested in G0/G1 were incubated in the

same medium with 10^{-9} M E2 or with 0.01% EtOH, as the vehicle control, for 3- to 6-hour intervals up to 36 hours. A fraction of cells at each time point was subjected to flow cytometry while the remaining was processed for WB analysis. E2 effectively triggered cell cycle progression such that the proportion of cells in the S phase began to increase at 12 hours reaching its maximum at 21 hours with corresponding decreases in the cell population accumulated in G0/G1. At subsequent time points, cells transited to the G2/M phase, completing the cycle by 30 hours with an increase in G0/G1 that resulted in a largely desynchronized cell population at 36 hours. In clear contrast, ethanol as the vehicle control did not affect cycle phase distribution as the majority of the cell population remained in the G0/G1 phase at every time point examined (Figure 2A & 2B).

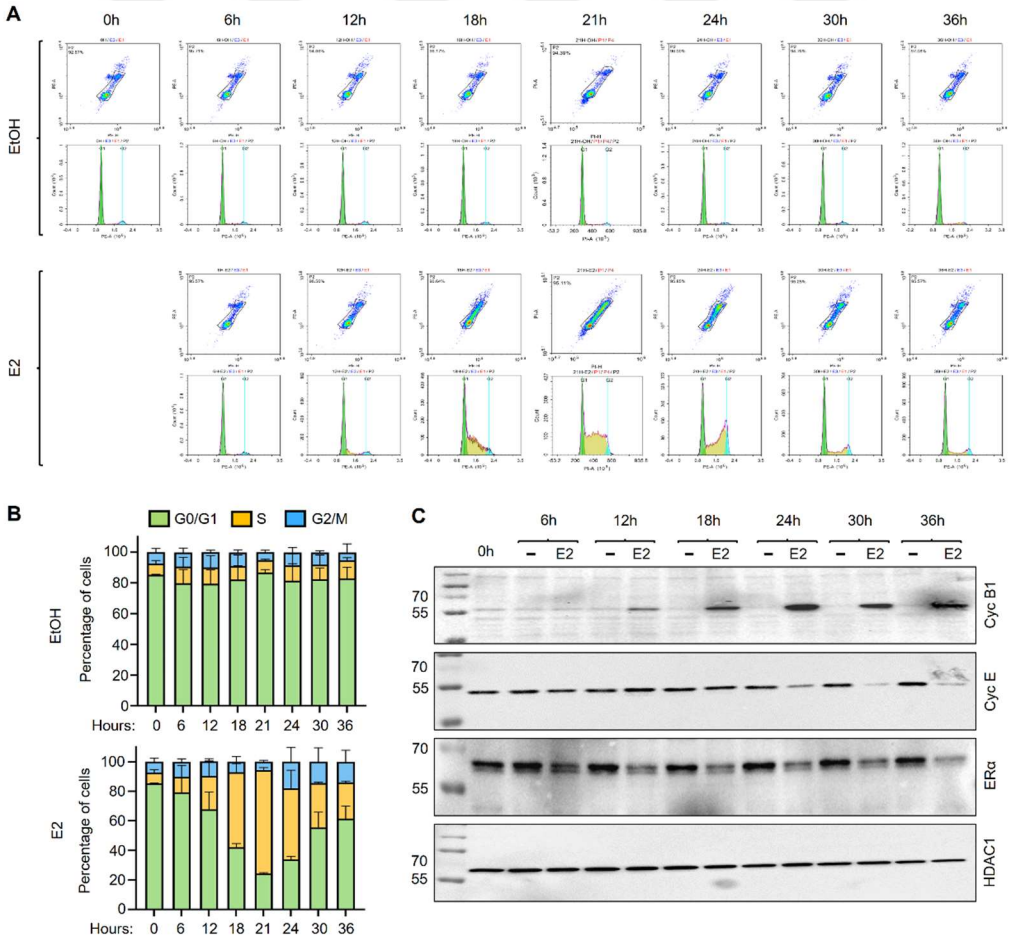

Figure 2. Effects of 17β-estradiol (E2) on cell cycle progression of MCF7 cells synchronized at G0/G1 by hormone withdrawal.

MCF7 cells were plated and grown in DMEM medium supplemented with 10% CD-FBS for 72h with media change at 48h. Cells were subsequently maintained in the same medium containing 0.01% ethanol (EtOH) as vehicle control or 10^{-9} M E2 for 3-6 h intervals up to 36h. At the termination, cells were collected with trypsinization. **(A)** A fraction of cells was subjected to the flow cytometry analysis **(B)** represented with a bar graph of two independent replicates, and **(C)** the remaining fraction was processed for WB analysis using an antibody for Cyclin B1 (Cyc B1), Cyclin E (Cyc E), ERα, or HDAC1. Molecular masses in kDa are indicated. In A & C, representative images from the same experiment conducted two independent times are shown. G0/G1, S, and G2/M indicate cell cycle phases.

The cell cycle progression triggered by E2 was also reflected in changes in protein levels of Cyclin B1 or Cyclin E, which were assessed with WB analysis (Figure 2C). Cyclin B1 is the regulatory subunit of cyclin-dependent kinase 1 (CDK1) and is essential for the transition from the G2 phase to mitosis[48]. On the other hand, Cyclin E is an activator of CDK2 (Cyclin-Dependent Kinase 2) and is critical for the entry to and progression through the S phase[49]. We observed that the protein levels of Cyclin B1 started to increase in the early S phase (at 12 hours of E2 treatment) and remained elevated until the cells were desynchronized, whereas Cyclin E began to decrease at the late S phase (24 hours) reaching low levels at 36 hours (Figure 2C). Consistent with previous studies which showed that E2 treatment rapidly decreases ERα levels[50–52], the E2 treatment of the synchronized MCF7 cells reduced ERα levels by 6 hours, which then remained at similar levels at the remainder of the cycle as assessed with HDAC1 as the loading control (Figure 2C). On the other hand, ERα levels remained unchanged at all time points in EtOH-treated cells. Thus, E2 acts as a mitogenic factor for MCF7 cells. These results indicate that the maintenance of cells in the growth medium supplemented with CD-FBS effectively synchronizes the cell cycle of MCF7 cells culminating in an enriched G0/G1 population.

3.1.1 E2-induced cell cycle progression and E2-ERα signaling

ERs also bind to various molecules with agonist, mixed agonist-antagonist, or full antagonist properties[53,54]. Mixed agonists/antagonists, also called “selective estrogen receptor modulators” (SERMs), display distinct pharmacological effects depending on the estrogen target tissue. For instance, tamoxifen (TAM) is a synthetic

nonsteroidal compound that has been widely used for the treatment of breast cancers as an antagonist, although it acts as an agonist in the uterus[53,54]. Pure antagonists of estrogenic compounds, such as Imperial Chemical Industries 182,780 (ICI), are steroidal analogs of estradiol, which are also referred to as the "selective estrogen receptor down-regulators" (SERDs), and act as complete antagonists[53,54]. Most of the key amino acids in the ligand-binding cavity of ERα that are responsible for binding TAM and ICI are the same. However, a large side chain emanating from the core of ICI causes a significant conformational shift in the ligand binding domain of ERα. This conformational change impairs dimerization and increases ERα degradation resulting in the prevention of target gene expressions[37,55,56].

To ensure that E2-induced cell cycle progression is dependent on ERα signaling, MCF7 cells were synchronized at G0/G1 with the growth medium containing 10% CD-FBS for 72 hours, then treated for 24 hours without or with 10^{-9} M E2 and/or 10^{-7} M ICI (also Supplementary Data, Figure 14D). ICI alone did not affect the cell population synchronized at the G0/G1 phase, but it effectively blocked the E2-mediated cell cycle progression assessed with the accumulation of cells in the S phase (Figure 3A). ICI also reduced the levels of ERα whether or not cells were treated with E2, as assessed with WB (Figure 3B). Thus, these observations indicate that the E2-ERα signaling is the primary pathway to induce cell cycle progression in MCF7 cells synchronized at G0/G1 in DMEM containing 10% CD-FBS for 72 hours.

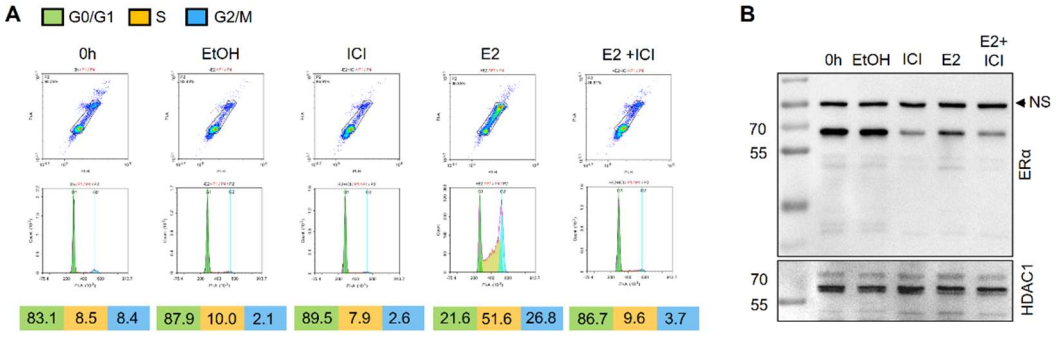

Figure 3. Effects of Imperial Chemical Industries 182780, ICI, on E2-induced cell cycle progression of MCF7 cells synchronized at G0/G1 by hormone withdrawal.

MCF7 cells synchronized at G0/G1 by the CD-FBS approach (0h) were treated without (0.01% EtOH) or with 10^{-9} M E2 and/or 10^{-7} M ICI for 24h. Cells were collected with trypsinization and **(A)** subjected to the flow cytometry analysis or **(B)** WB using an antibody for ERα or HDAC1. Representative images from the same experiment conducted two independent times are shown. G0/G1, S, and G2/M indicate cell cycle phases. NS indicates a nonspecific protein species detected with the ERα antibody.

3.2 Synchronization of the Cell Cycle of MCF7 Cells with Double Thymidine Block (DTB) Approach

Various chemicals including lovastatin and mimosine have been used for cycle synchronization at the G1 phase. Lovastatin is a 3-hydroxy-3-methylglutaryl-coenzyme A reductase (HMG-CoA reductase) inhibitor and results in G1 cell cycle arrest by inducing CDKIs such as p21 and p27[57,58]. The addition of mevalonate, which increases the degradation of the CDKIs through an increased proteasome activity[59], drives the release of cells from the G1 arrest for entry into the S and G2/M phases of the cell cycle[60]. Mimosine, which is a rare plant amino acid, reversibly arrests the progression of the cell cycle at G1 before the onset of DNA replication[61,62]. On the other hand, double thymidine block (DTB) is a widely utilized chemical technique that relies on the interruption of the deoxynucleotide metabolism pathway through competitive inhibition with excess thymidine, and it arrests cells at the G1/S boundary before DNA replication[29,63–65].

Based on variable results with lovastatin and mimosine in our earlier explorations, we selected to use the DTB approach[29] to synchronize MCF7 cells as an alternative method to the CD-FBS treatment. To assess the effects of DTB, MCF7 cells grown in DMEM containing 10% FBS were subjected to DTB with an initial 2 mM thymidine treatment for 14 hours followed by a release from thymidine for 12 hours and re-blocking with 2 mM thymidine for 22 hours. The DTB approach synchronized MCF7 cells at the G1/S border with a substantial population of cells also present at the beginning of the S phase, as reported previously[66], independently of thymidine concentrations we tested (2-10 mM) (Figure 4A & 4B; Supplementary Data, Figure 15). Nevertheless, the release from DTB (RDTB) rapidly drove the progression of

cells through the S phase within 6 hours. Cells transited to G2 at 8 hours after the release from DTB and subsequently desynchronized at 14 hours (Figure 4A & 4B). The cycle phase transitions were also reflected in high levels of Cyclin E at the beginning of the release from DTB which started to decline in the late S phase reaching steady-state levels until the desynchronization of cells. On the other hand, the levels of Cyclin B1 began to increase at the progression of the S phase and sharply declined as the cells desynchronized to levels similar to those observed with unsynchronized cells. Whereas ERα levels remained primarily unchanged throughout the cycle as the protein levels of HDAC1, which was used as the loading control (Figure 4C).

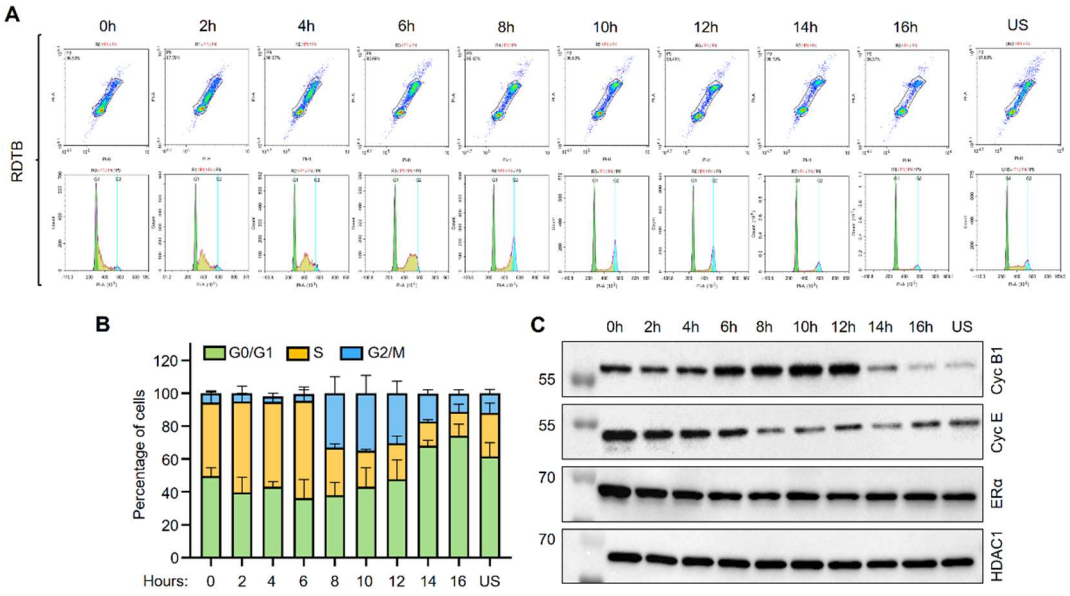

Figure 4. Cell cycle progression following the release of synchronized MCF7 cells from double thymidine block. MCF7 cells maintained in DMEM medium supplemented with 10% FBS were incubated in the same medium containing 2 mM thymidine for 14h. Cells were then released from thymidine treatment by twice washing the cells with 1x PBS and re-incubating them in DMEM medium containing 10% FBS without thymidine for 12h. Cells were subsequently washed and incubated with the same medium containing 2 mM thymidine for 22h. Cells were released from the double thymidine block (RDTB) by freshening the culture medium (0h). Cells were collected with trypsinization at 2h intervals for 16h following release and **(A)** subjected to flow cytometry analysis **(B)** with the result of two independent experiments represented with a bar graph. **(C)** Cells were also prepared for and subjected to WB using antibodies for Cyclin B1 (Cyc B1), Cyclin E (Cyc E), ERα, or HDAC1. Molecular masses in kDa are indicated. In A & C, representative images from the same experiment replicated two independent times are presented. G0/G1, S, and G2/M indicate cell cycle phases. US indicates unsynchronized cells.

3.2.1 Combination of DTB with CD-FBS synchronization

To examine whether the accumulation of cells at the G1/S transition as well as cell cycle progression following the release of DTB requires the presence of E2, we assessed the combination of DTB and CD-FBS on cell cycle synchronization. For this, MCF7 cells maintained in DMEM containing 10% FBS for 72 hours were washed and incubated in DMEM supplemented with 10% CD-FBS containing 2 mM thymidine for 14 hours. Cells were subsequently released from the thymidine block with DMEM containing 10% CD-FBS for 12 hours. Cells were re-incubated with DMEM medium containing 10% CD-FBS and 2 mM thymidine for 22 hours. For the release, cells were treated with 10^{-9} M E2 or with 0.01% EtOH in DMEM containing 10% CD-FBS for 2- to 4-hour intervals up to 32 hours. This approach effectively synchronized the cells in G0/G1 as more than 80% of the cell population accumulated in the G0/G1 phase at the time of the release (0h) from the DTB (Figure 5A & 5B) as similarly observed with the CD-FBS treatment (Figure 2A & 2B). Following the DTB release, the presence of E2 triggered cell cycle progression, although with a substantial delay compared to DTB alone but similar to those observed with the CD-FBS approach. We observed that E2 treatment-coupled DTB release initiated the cell cycle progression with cells entering the S phase by 12 hours, reaching a maximal population by 20 hours, and exiting the S phase by 24 hours with eventual desynchronization of the cycle at 32 hours (Figure 5A & 5B). Cell cycle progression was correlated with Cyclin B1 levels which showed an increase at the beginning of the S phase and remained at high levels thereafter. In contrast, protein levels of Cyclin E declined with the S phase. ERα levels also decreased upon E2-triggered cell cycle progression whereas the levels of HDAC1, used as the loading control, remained unchanged (Figure 5C).

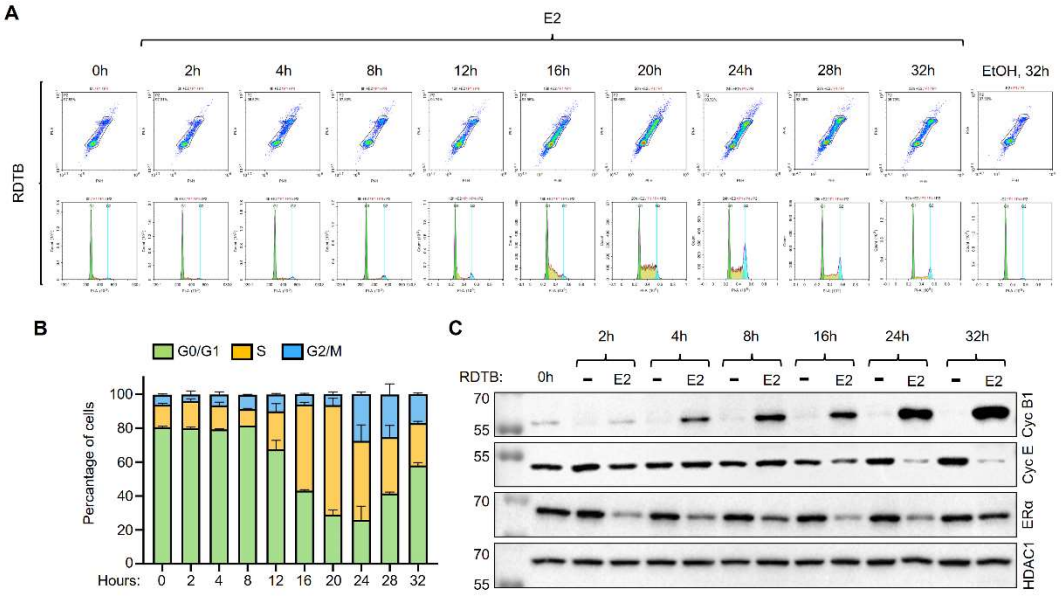

Figure 5. Effects of 17β-estradiol (E2) on cell cycle progression of MCF7 cells synchronized at G0/G1 by hormone withdrawal and double thymidine block. MCF7 cells grown in DMEM medium supplemented with 10% FBS in T-25 tissue culture flasks for 72h were washed and incubated in the fresh medium containing 10% CD-FBS together with 2 mM thymidine for 14h. Cells were then released from thymidine treatment by washing the cells with 1x PBS and re-incubating them in DMEM medium containing 10% CD-FBS without thymidine for 12h. Cells were subsequently washed and incubated with DMEM medium containing 10% CD-FBS and 2 mM thymidine for an additional 22h. Cells were released from the double thymidine block (RDTB) by washing the cells and incubating them with DMEM medium containing 10% CD-FBS in the absence (0.01% EtOH) or presence of 10^{-9} M E2 for 2-4 h intervals up to 32h. At the termination at each time point, cells were collected with trypsinization. **(A)** A fraction of cells was subjected to flow cytometry analysis **(B)** with a bar graph representing the results of two independent experiments, and **(C)** the remaining fraction of cells was processed for WB using an antibody for Cyclin B1 (Cyc B1), Cyclin E (Cyc E), ERα, or HDAC1. In A & C, representative images from the same experiment conducted two independent times are shown. G0/G1, S, and G2/M indicate cell cycle phases.

3.2.2 E2 treatment-coupled DTB release and E2-ERα signaling

To ensure that E2 treatment-coupled DTB release is dependent on ERα signaling, MCF7 cells synchronized at G0/G1 with the DTB approach in the growth medium containing 10% CD-FBS were treated for 24 hours without or with 10^{-9} M E2 and/or 10^{-7} M ICI at the time of release. ICI alone did not affect the G0/G1 phase population, but it effectively blocked the cell cycle progression assessed with the accumulation

of cells in the S phase following release from DTB induced by E2 (Figure 6A). ICI also reduced the levels of ERα whether or not cells were treated with E2 (Figure 6B). Thus, the E2-ERα signaling is the primary factor in driving cell cycle progression in MCF7 cells synchronized at G0/G1 with CD-FBS alone or in combination with DTB.

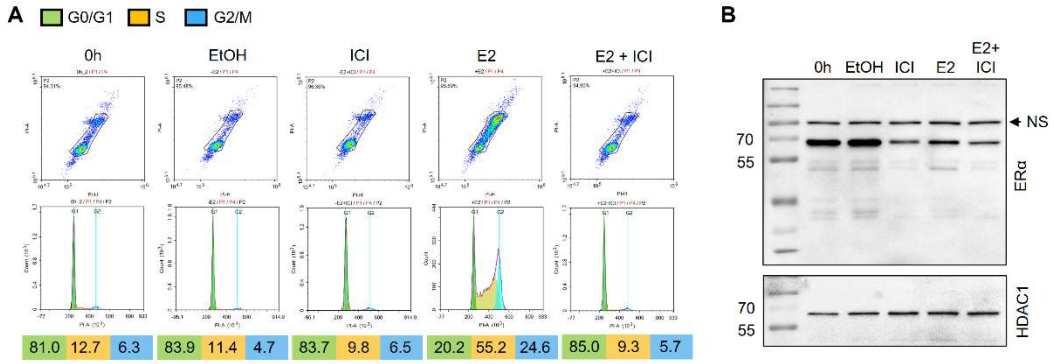

Figure 6. Effects of ICI on E2-induced cell cycle progression of MCF7 cells synchronized at G0/G1 by hormone withdrawal and double thymidine block. MCF7 cells synchronized at G0/G1 by CD-FBS and double thymidine block were treated without (0.01% EtOH) or with 10^{-9} M E2 and/or 10^{-7} M ICI for 24h. **(A)** Cells were collected with trypsinization and subjected to the flow cytometry analysis or **(B)** WB using an antibody for ERα or HDAC1. Representative images from the same experiment are shown. G0/G1, S, and G2/M indicate cell cycle phases. NS designates a nonspecific protein species detected with the ERα antibody. Molecular masses in kDa are indicated.

3.3 Synchronization of Cell Cycle using Antiestrogens in MCF7 Cells

Antiestrogens including 4-HTam and ICI block the cycle of MCF7 cells[33,67–70] and the block can be reversed by E2 resulting in a synchronized cohort of cells progressing through the S phase[67]. This raises the possibility that the withdrawal of antiestrogens could drive the cell cycle progression of synchronized cells at G0/G1 maintained in the complete growth medium. This approach could generate a simplified experimental model necessitating the use of only antiestrogens for the synchronization of MCF7 cells. To assess this possibility, we treated unsynchronized MCF7 cells maintained in DMEM medium containing 10% FBS without or with 10^{-7} M 4-HTam or ICI (Supplementary Data, Figure 14) for 48 hours, the duration of

which was based on our observations that MCF7 cells complete cell cycle within 36 hours (Figure 2A). Both compounds effectively synchronized MCF7 cells at the G0/G1 phase (Figure 7A & 7D). Nevertheless, the treatment of cells with ICI was more effective in the accumulation of cells at G0/G1 (% 84 ± 1.5) compared to the 4-HTam treatment (% 72 ± 3). The release from the block by incubating cells in the fresh growth medium without 4-HTam or ICI (post-release, PR) for up to 72 hours did not allow cells to transit cycle phases.

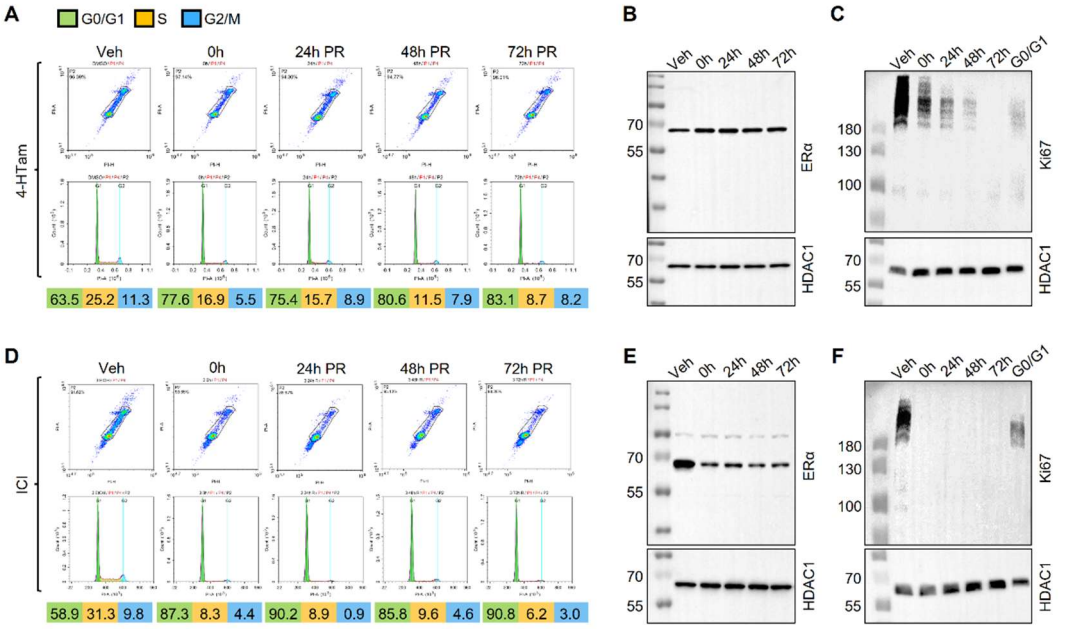

Figure 7. Effects of 4-Hydroxytamoxifen, 4-HTam, or Imperial Chemical Industries 182780, ICI, on the synchronization and progression of cycle phases of MCF7 cells. MCF7 cells maintained in DMEM medium supplemented with 10% FBS were incubated in fresh media containing 0.0002% DMSO or 0.01% EtOH as vehicle control or **(A-C)** 10^{-7} M 4-HTam or **(D-F)** ICI respectively for 24h. Cells were washed with 1x PBS and either immediately collected (0h) by trypsinization or maintained in DMEM medium supplemented with 10% FBS (post-release, PR) at 24h intervals for 72h with a medium change at 48h and subsequently collected by trypsinization. **(A & D)** A fraction of collected cells was subjected to flow cytometry analysis, and **(B & C** and **E & F)** the remaining cells were subjected to WB using an antibody specific for ERα, HDAC1, or Ki67. Molecular masses in kDa are indicated. G0/G1, S, and G2/M indicate cell cycle phases. Representative images from the same experiment replicated two independent times are shown.

We observed that cells synchronized at G0/G1 by the 10^{-7} M 4-HTam treatment for 48 hours remained at G0/G1 and the percentage of G0/G1 population increased in a

time-dependent manner without alteration in ERα levels (Figure 7A & 7B). Instead, the percentage of 10^{-7} M ICI pre-treated cells accumulated at G0/G1 remained the same throughout the experimental period (Figure 7D). ICI pre-treatment, as expected, reduced ERα levels as assessed with WB (Figure 7E).

A previous study suggested that ICI-mediated cell cycle arrest of MCF7 cells at G0/G1 have characteristics of G0 rather than the G1 phase[71]. Ki67, also known as the Marker of Proliferation Ki-67 (MKI67), is strictly associated with cell proliferation. Ki67 protein is present during all active phases of the cell cycle (G1, S, G2, and M), but is absent from resting cells (G0)[72,73]. This stage-specific synthesis of Ki67 has been used as a marker for active cell proliferation[72,73]. WB analysis of MCF7 cells pre-treated with ICI using an antibody specific to Ki67 as a marker for proliferation revealed that Ki67 synthesis was indeed undetectable compared to unsynchronized vehicle-treated control cells (Figure 7F). On the other hand, Ki67 levels in 4-HTam pre-treated MCF7 cells showed a time-dependent decline that was inversely correlated with an increase in the percentage of cells accumulated in G0/G1 throughout the experimental duration (Figure 7C). Thus, as suggested previously for ICI[71], antagonist treatment of exponentially growing MCF7 cells in the complete medium results in a quiescent state of cells unresponsive to the removal of the compound.

3.4 Enrichment of Cell Cycle Phases by E2 Treatment-Coupled Chemical Agents in MCF7 Cells

Based on our results that CD-FBS effectively synchronizes MCF7 cells in G0/G1 and the replacement of E2 efficiently drives cycle progressions, we wanted to assess whether we could also obtain cell populations enriched specifically at S, G2, and/or M phases with various chemical agents.

3.4.1 Enrichment of the S phase

Aphidicolin is a tetracyclic diterpenoid that reversibly inhibits functions of DNA polymerase α, δ, and ε arresting cell cycle progression at the G1/S transition thereby blocking DNA synthesis in cells that have entered S-phase[30]. Therefore, we reasoned that the co-treatment of E2-treated cells with aphidicolin could enrich the population in the S phase dependent upon the duration of E2 treatment. To test this prediction, we used 10 μM of aphidicolin at different time points of the S phase following the E2 treatment of MCF7 cells synchronized at G0/G1. We observed no significant effect of aphidicolin at this, or other concentrations[38] on the S phase population at any point we tested (Supplementary Data, Figure 16A & 16B). Similarly, 2,3-DCPE, which is a synthetic compound suggested to induce S phase arrest by activating the ATM/ATR-Chk1-Cdc25A signaling pathway in DLD-1 colon cancer cells[39,74], was utilized for S phase enrichment. Based on previous studies in our laboratory[38], MCF7 cells were treated without or with 20 μM 2,3-DCPE 6 hours after E2 treatment of MCF7 cells synchronized at G0/G1, however, 2,3-DCPE did not further enrich the S phase population of MCF7 cells generated by E2 treatment (Supplementary Data, Figure 16C).

These results suggest that harvesting cells at a specific time point corresponding to the highest population of MCF7 cells accumulated in the S phase, the 21-hour E2 treatment as our results indicate, is the best option for the S phase enrichment.

3.4.2 Enrichment of the G2/M phase

Despite the effective synchronization by CD-FBS and subsequent progression through cycle phases by E2 treatment of MCF7 cells, the rapid progression through the G2/M phase for the cycle completion does not generate a significantly enriched cell population at the G2/M phase. Nocodazole is an anti-mitotic agent that, depending on the concentration, either interferes with the tubulin exchange dynamics at microtubule ends or depolymerizes microtubules by binding to β-tubulin[75]. This

in turn can impair the microtubule-kinetochore attachment or the formation of the metaphase spindles during the cell division cycle, thereby arresting cells in G2/M leading to the prevention of mitosis[75]. Nocodazole-treated cells can also be harvested by mitotic shake-off to generate a high percentage of cells at the M phase. Mitotic shake-off exploits the decreased membrane surface area of spherical mitotic cells attached to the culture plate, hence allowing the detachment of cells by gentle shaking[76]. To enrich the G2/M population, MCF7 cells synchronized at G0/G1 by the CD-FBS approach were treated with 10^{-9} M E2 for varying durations to enrich the cell population in different stages (entrance, accumulation, and exit) of the S phase (Supplementary Data, Figure 17). Cells were then subjected to various concentrations of nocodazole for 6 hours in the absence or presence of E2.

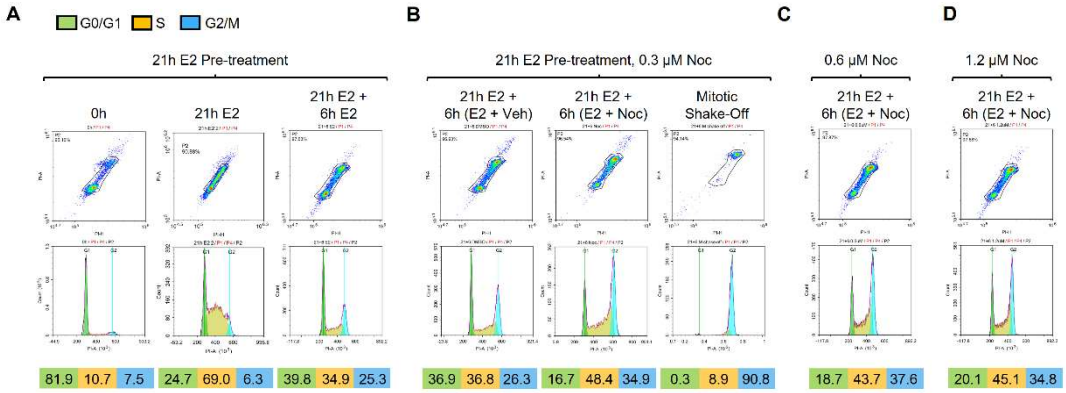

Figure 8. Effects of various concentrations of nocodazole (Noc) on the G2/M or M phase in synchronized MCF7 cells progressed to the S phase in response to the E2 treatment. MCF7 cells were grown in DMEM medium supplemented with 10% CD-FBS for 72h. Cells were either collected by trypsinization (0h) or treated in the same medium with 10^{-9} M E2 for 21h. Cells were then washed and incubated in the same medium containing **(A)** 10^{-9} M E2, **(B)** and/or 0 (Veh), 0.3, **(C)** 0.6 or **(D)** 1.2 µM nocodazole (Noc) for an additional 6h. Cells were either subjected to trypsinization or mitotic shake-off for collection and subjected to flow cytometry. Representative images with cell cycle phases from the same experiment conducted two independent times are presented.

We observed that nocodazole treatment of cells, independently of concentrations, at 21 hours of E2 treatment further enriched the G2/M phase population (Figure 8). Moreover, we obtained a nearly pure population of cells (≥90 %) in the M phase by nocodazole-coupled mitotic shake-off (Figure 8B). It should be cautioned that the

size of the M phase population obtained with mitotic shake-off is substantially lower compared to other phases, requiring the initial use of a large number of cells for specific M phase enrichment.

In conclusion, nocodazole alone or nocodazole-coupled mitotic shake-off could be used for the enrichment of the G2/M phases or M phase, respectively, of the cell cycle induced by E2 in MCF7 cells.

3.5 Enrichment of Cell Cycle Phases using Various Approaches in T47D Cells

Although MCF7 and T47D cells are derived from a metastatic site of pleural effusion, they display distinct molecular characteristics and cell cycle profiles[11–14,77]. Therefore, we wanted to assess whether T47D cells could be synchronized, and cell cycle phase enriched with approaches we employed for MCF7 cells.

3.5.1 Synchronization of the cell cycle of T47D cells with CD-FBS with or without E2 replacement

To examine the effectiveness of the CD-FBS approach on cell cycle synchronization of T47D cells, T47D cells grown in the RPMI 1640 medium supplemented with 10% CD-FBS for 72 hours were treated with 10^{-9} M E2 or with 0.01% EtOH for 6-hour intervals up to 36 hours. As we observed with MCF7 cells, CD-FBS synchronized T47D cells efficiently in the G0/G1 phase (85%). The supplementation of the medium with 10^{-9} M E2 induced cell cycle progression of T47D cells in a time-dependent manner, where the S phase population started to slightly increase at 18 hours of E2 treatment. However, E2 drove only a small fraction of the G1 phase population into cycle progression such that the maximal percentage of cell population accumulated in the S phase at 24 hours was less than 25%. The S phase cell population subsequently traversed to G2/M and desynchronized at 36 hours (Figure 9A & 9B).

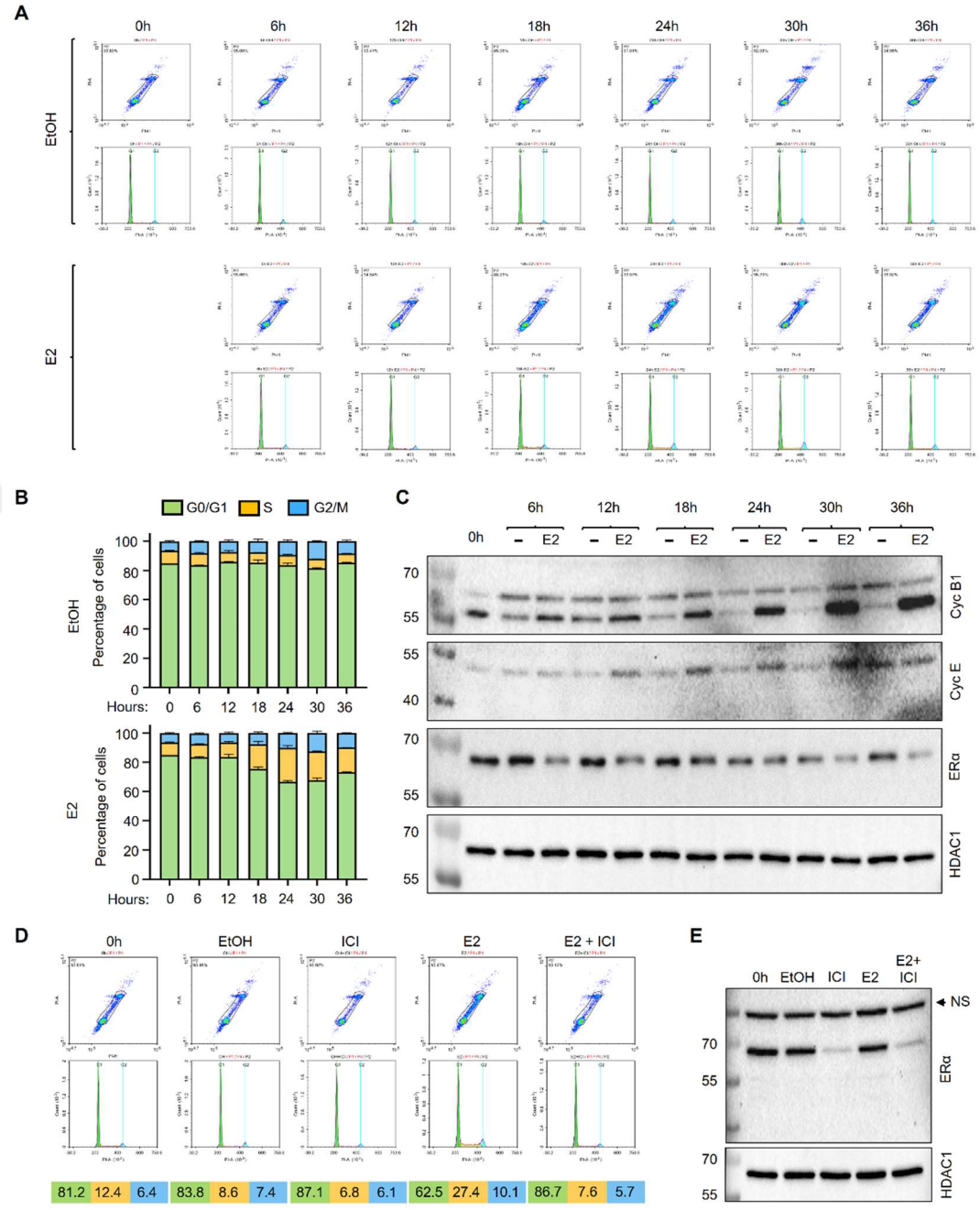

Figure 9. Effects of 17β-estradiol (E2) on cell cycle progression of T47D cells synchronized at G0/G1 by hormone withdrawal.

T47D cells were plated and grown in RPMI 1640 medium supplemented with 10% CD-FBS for 72h with the medium change at 48h. **(A-C)** Cells were subsequently maintained in the same medium containing 0.01% ethanol (EtOH) as vehicle control or 10^{-9} M E2 for 6h intervals up to 36h. Cells were collected with trypsinization. **(A)** A fraction of collected cells was subjected to the flow cytometry analysis **(B)** the results of which are represented with a bar graph of two independent replicates, and **(C)** the remaining cells were processed for WB analysis using an antibody for Cyclin B1 (Cyc B1), Cyclin E (Cyc E), ERα, or HDAC1. Molecular masses in kDa are indicated. **(D & E)** T47D cells synchronized at G0/G1 by hormone withdrawal (0h) were treated without (0.01% EtOH) or with 10^{-9} M E2 and/or 10^{-7} M ICI for 24h. **(D)** Cells were collected with trypsinization and subjected to flow cytometry or **(E)** WB using an antibody for ERα or HDAC1. In A & C and D & E, representative images from the same experiment are shown. G0/G1, S, and G2/M indicate cell cycle phases. Molecular masses in kDa are indicated. NS designates an unspecific protein species detected with the ERα antibody.

These phase transitions were correlated with the levels of Cyclin E and B1 assessed with WB. E2 treatment of cells rapidly reduced ERα levels in 6 hours as expected, which then remained at low levels in contrast to the loading control HDAC1, with levels similar throughout the cell cycle (Figure 9C).

To assess whether E2-induced cell cycle progression of T47D cells is also dependent on ERα signaling like MCF7 cells, T47D cells were synchronized at G0/G1 with the growth medium containing 10% CD-FBS for 72 hours, then treated for 24 hours without or with 10^{-9} M E2 and/or 10^{-7} M ICI. When given together with E2, ICI prevented the accumulation of cells in the S phase at 24 hours (Figure 9D). ICI also decreased ERα levels in the presence or absence of E2 as assessed with WB (Figure 9E). Therefore, it can be concluded that the cell cycle progression of T47D cells induced by E2 is ERα-mediated.

3.5.2 Combination of DTB with CD-FBS synchronization

To assess the combination of DTB and CD-FBS on cell cycle synchronization of T47D cells, cells grown in the RPMI 1640 medium containing 10% FBS for 72 hours were washed and incubated in RPMI 1640 supplemented with 10% CD-FBS containing 2 mM thymidine for 14 hours. Cells were then refreshed with RPMI 1640 containing 10% CD-FBS for 12 hours for release from the thymidine block. Cells

were re-incubated with the RPMI 1640 medium containing 10% CD-FBS and 2 mM thymidine for 22 hours. For the release, cells were treated with 10^{-9} M E2 or with 0.01% EtOH in RPMI 1640 containing 10% CD-FBS for 2- to 4-hour intervals up to 32 hours. Synchronization of T47D cells with this approach partially synchronized T47D cells at the G1 phase (0h) with a substantial cell population (29 + 1.8%) present at the G1/S transition (Figure 10A & 10B). The release from DTB with a concomitant supplementation of the medium with E2 drove the cells accumulated at G1 and/or G1/S transition to progress through the S phase in 4 hours and transit to the G2/M phase at 8 hours, completing their cell cycle at 12 hours (Figure 10A & 10B).

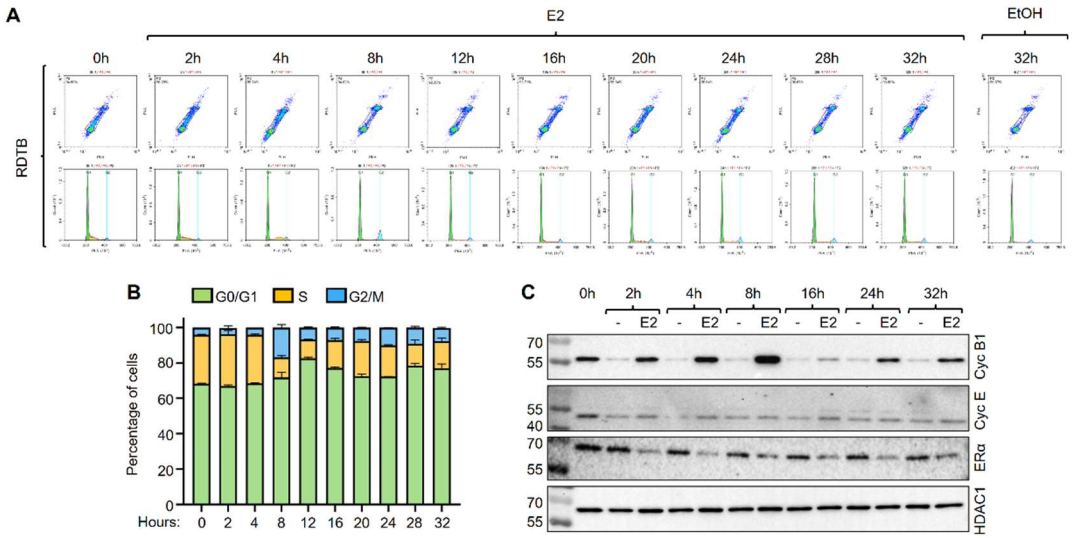

Figure 10. Effects of 17β-estradiol (E2) on cell cycle progression of T47D cells synchronized at the G1/S transition by CD-FBS and double thymidine block. T47D cells grown in RPMI 1640 medium supplemented with 10% FBS for 72h were incubated in RPMI 1640 medium containing 10% CD-FBS together with 2 mM thymidine for 14h followed by washing the cells and re-incubating in the same medium without thymidine for 12h. Cells were re-incubated with fresh RPMI 1640 medium containing 10% CD-FBS and 2 mM thymidine for an additional 22h. Cells were released from the double thymidine block (RDTB) by washing the cells and incubating with the same medium in the absence (0.01% EtOH) or presence of 10^{-9} M E2 for 2-4 h intervals up to 32h. Cells at each time point were collected with trypsinization and **(A)** subjected to flow cytometry **(B)** with a bar graph representing the results of two independent experiments, and **(C)** to WB using antibodies for Cyclin B1 (Cyc B1), Cyclin E (Cyc E), ERα, or HDAC1. In A & C, representative images from the same experiment are shown. G0/G1, S, and G2/M indicate cell cycle phases. Molecular masses in kDa are indicated.

This cell cycle phase progression was also reflected in Cyclin B1 and Cyclin E levels in WB analyses. Cyclin B1 levels increased through 8 hours after release from DTB as the cells progressed to the G2/M phase, then dropped after the cells became desynchronized. ERα levels were rapidly reduced in response to E2 treatment, and they remained low throughout the cell cycle, whereas HDAC1 levels as the loading control remained unchanged (Figure 10C).

3.5.3 Synchronization with DTB approach and S phase enrichment

It appears that although E2-ERα signaling contributes to the cell cycle progression of T47D cells, it is not sufficient to drive the large population of cells synchronized with DTB in the growth medium supplemented with CD-FBS to transit through cell cycle phases. This in turn suggests that in addition to estrogens, CD treatment of FBS also removes components critical for T47D cell proliferation. To test this possibility, we employed the DTB approach on T47D cells grown in the RPMI 1640 medium supplemented with 10% FBS. We indeed observed that DTB partially synchronized the cells at G1 and the G1/S transition (0h) with a substantially higher percentage (45 + 1.5%) of cells compared to that observed with the DTB combined with the CD-FBS approach (29 + 2%). The withdrawal of DTB effectively released T47D cells accumulated at G1 and G1/S to progress through the S phase in 4 hours, then start transiting to the G2/M phase in 6 hours and completing the cycle in 12 hours (Figure 11A & 11B). In parallel with the cell cycle phase distributions, Cyclin B1 levels gradually increased until 6 hours as the cells transited to the G2/M phase, then started decreasing as the cells exited G2/M and became desynchronized. Cyclin E levels were reduced as soon as the cells progressed through the S phase and continued their cycle progression, whereas levels of ERα were not affected similar to HDAC1 (Figure 11C).

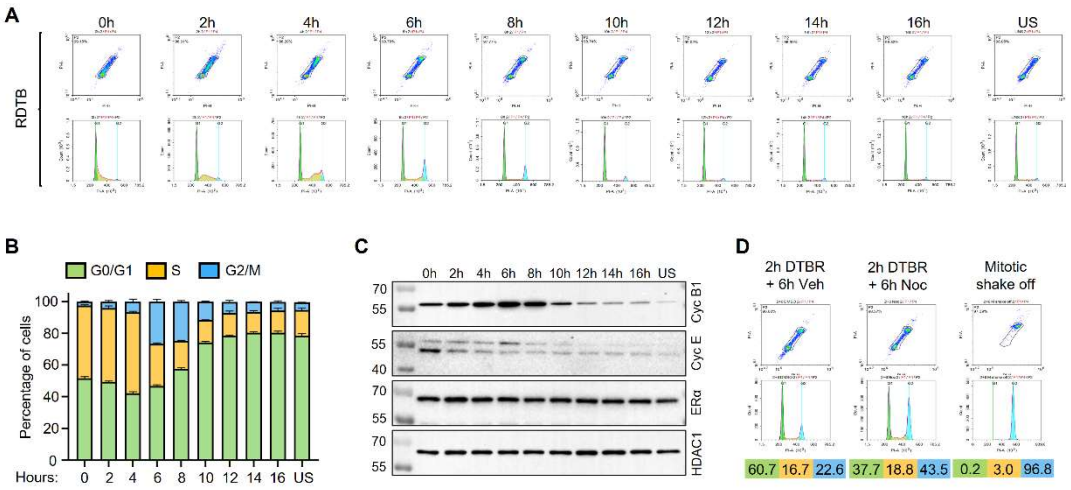

Figure 11. Effects of the release of T47D cells from double thymidine block on cycle progression and phase enrichment. T47D cells were grown in RPMI 1640 medium supplemented with 10% FBS for 72h. Cells were incubated with RPMI 1640 medium supplemented with 10% FBS and with 2 mM thymidine for 14h. Cells were released from the thymidine block in the same medium without thymidine for 12h. Cells were re-incubated with fresh RPMI 1640 medium containing 10% FBS and 2 mM thymidine for an additional 22h. Cells were subsequently released from the double thymidine block (RDTB) and incubated in the same growth medium without thymidine for 2h intervals up to 16h. Cells at each time point were collected with trypsinization and **(A)** subjected to flow cytometry analysis **(B)** with a bar graph representing the results of two independent experiments, and **(C)** to WB using an antibody for Cyclin B1 (Cyc B1), Cyclin E (Cyc E), ERα, or HDAC1. In A & C, representative images from the same experiment are shown. G0/G1, S, and G2/M indicate cell cycle phases. Molecular masses in kDa are indicated. US denotes unsynchronized cells. **(D)** T47D cells at 2h release from the double thymidine block (RDTB) were incubated in fresh RPMI 1640 medium containing 10% FBS without (Veh) or with 0.3 μM nocodazole (Noc) for an additional 6h. Cells were then collected by trypsinization or by mitotic shake-off for flow cytometry analysis. G0/G1, S, and G2/M indicate cell cycle phases.

Thus, while the CD-FBS approach effectively synchronizes T47D cells at the G0/G1 phase, E2 alone is insufficient to drive the large population of cells accumulated at G0/G1 to transit through phases for cell cycle completion. On the other hand, the DTB approach combined with CD-FBS partially synchronizes cells at G1 with a large population of cells remaining at the G1/S transition in a manner observed with DTB alone. Nevertheless, the enrichment of the S phase population could be achieved following the release of the cells from DTB alone.

3.5.4 G2/M phase enrichment with nocodazole

We also examined whether we could further enrich the G2/M or M phase population with the nocodazole treatment of T47D cells synchronized with DTB. T47D cells were treated with nocodazole at 2 hours of DTB release, which was based on the preliminary studies in which 2 hours post-DTB release was the optimal time for nocodazole to enrich cells in G2/M in 6 hours (Supplementary Data, Figure). We observed that nocodazole compared with vehicle control (DMSO) enriched the G2/M phase population (Figure 11D). Furthermore, nocodazole-coupled mitotic shake-off yielded a nearly pure M-phase population (≥90 %) (Figure 11D). Thus, as with MCF7 cells, nocodazole alone or together with mitotic shake-off can be used for the enrichment of the G2/M or M phase in synchronized T47D cells.

CHAPTER 4

CONCLUSION AND FUTURE DIRECTIONS

Breast cancer comprises a heterogeneous group of tumors displaying dramatic variations in clinical presentation, morphology, molecular features, biological behavior, and response to therapy[78–80]. Breast cancer is categorized into clinical subtypes primarily by receptor expression statuses[78–80]. ERα is a predominant endocrine regulatory protein in the breast tissue and in estrogen-induced breast cancer that accounts for more than 70% of cases. The current modalities for the treatment of ER-positive breast cancer are centered on agents with diverse pharmacology to reduce/ablate the circulating estrogens or to alter/prevent ER function. Approaches to perturb the estrogen signaling are usually successful in the remission of established tumors. However, many breast tumors eventually develop resistance to endocrine therapies[16,81].

Despite being prone to genetic and phenotypic alterations due to growth conditions and the evolution of clonal populations over time[11,77,82,83], breast cancer cell lines have been invaluable in vitro model systems for gaining mechanistic insight into cellular phenotype, drug discovery, and resistance. Of the large number of E2-responsive ERα-synthesizing breast cancer cell lines with distinct features[14,77,84], MCF7 and T47D cells have been widely used for a better understanding of integrated molecular events that coordinate cellular proliferation in response to the E2-ERα signaling.

Our previous attempts to delineate the contribution of proteostasis to genomic events mediated by the E2-ERα signaling in cycle phase enriched populations of synchronized MCF7 or T47D cells with various chemical/pharmacological agents yielded variable and unreliable results. Therefore, in this study, we reassessed cell cycle synchronization-coupled phase enrichment with CD-FBS alone or in

combination with the DTB approach or chemical/pharmacological agents in MCF7 and T47D cells. Based on the results we obtained from our experiments on MCF7 and T47D cells we conclude that:

1. The maintenance of MCF7 cells in the growth medium supplemented with CD-FBS and subsequent progression of cell cycle phases with the supplementation of the same growth medium with E2 is the most effective approach for cell cycle synchronization and synchronization-coupled cycle phase enrichment.
    a. MCF7 cells maintained in CD-FBS containing growth medium for 72 hours accumulated effectively in the G0/G1 phase with more than 80% of the cell population.
    b. The treatment of MCF7 cells synchronized at G0/G1 with E2 for 21 hours led to the S phase enrichment with almost 65% of the cells.
    c. The cells progressed to the G2/M phase at 24 hours of E2 treatment, however, the rapid progression through the G2/M phase for the cycle completion did not generate a significantly enriched cell population at the G2/M phase. This necessitated the use of chemical/ pharmacological agents for the enrichment of the G2/M phase.
    d. The treatment of MCF7 cells synchronized at G0/G1 without or with E2 and/or ICI for 24 hours showed that the E2-ERα signaling is the primary pathway to induce cell cycle progression in MCF7 cells synchronized at G0/G1 in DMEM containing CD-FBS for 72 hours.
2. The DTB approach synchronized MCF7 cells at the G1/S border with a substantial population of cells also present at the beginning of the S phase. The release from DTB rapidly drove the progression of cells through the S and G2/M phases with subsequent desynchronization at 14 hours. Although the DTB approach successfully synchronizes the cells at the G1/S border, it

is not the most ideal method for enrichment of the G1 phase if a highly enriched population is desired.

3. The combination of DTB and CD-FBS effectively synchronized the cells in G0/G1 as more than 80% of the cell population accumulated in the G0/G1 phase at the time of the release from the DTB, and E2 treatment-coupled DTB release induced the cell cycle progression, similar to what we observed with the CD-FBS treatment. The treatment of MCF7 cells synchronized at G0/G1 with the DTB approach in the growth medium containing CD-FBS without or with E2 and/or ICI revealed that the E2-ERα signaling is the primary factor in driving cell cycle progression in MCF7 cells synchronized at G0/G1 using DTB in combination with CD-FBS.

4. The antiestrogens 4-HTam and ICI both effectively synchronized MCF7 cells at the G0/G1 phase, although the treatment of cells with ICI was more effective in the accumulation of cells at G0/G1 compared to 4-HTam treatment. However, we were not successful in driving the cell cycle progression after withdrawing the 4-HTam or ICI from the culture medium. Our flow cytometry and WB results indicate that the treatment of the cells with 4-HTam or ICI drove them to a quiescent state of cells unresponsive to the removal of the compound.

5. Using aphidicolin or 2,3-DCPE in combination with CD-FBS treatment and E2 supplementation for the enrichment of the S phase gave variable results that were not reliable. Thus, harvesting cells at a specific time point corresponding to the highest population of MCF7 cells accumulated in the S phase, the 21-hour E2 treatment as our results indicate, is the best option for the S phase enrichment.

6. Nocodazole treatment of MCF7 cells at the S phase following 21 hours of E2 treatment for 6 hours augmented the G2/M phase population; whereas, nocodazole-coupled mitotic shake-off yielded a nearly pure population in the M phase.

7. Similar to the MCF7 cells, the CD-FBS approach effectively synchronized T47D cells at G0/G1, and the E2 treatment initiated cycle phase transitions. However, a small population of cells, in contrast to MCF7 cells, accumulated in G0/G1 progressed through cell cycle phases in response to E2, rendering the enrichment of S and/or G2/M phases with the CD-FBS approach difficult. This suggests that other serum factors alongside estrogens removed by the CD treatment critically contribute to the proliferation of T47D cells. Nevertheless, the treatment of T47D cells synchronized at G0/G1 without or with E2 and/or ICI revealed that the cell cycle progression of T47D cells induced by E2 is ERα-mediated.

8. Synchronization of T47D cells with the DTB approach increased the cell population in the S phase at 2 hours of release following DTB whether or not cells are maintained in CD-FBS. Nevertheless, the DTB approach without CD-FBS yielded a more effective S phase enrichment compared to the DTB combined with CD-FBS, although the presence of a substantial population at the early S phase following the release of cells from DTB poses challenges for the G1 enrichment.

9. Nocodazole alone or together with mitotic shake-off can be used for the enrichment of the G2/M or M phase, respectively, of T47D cells synchronized with the DTB approach, where 2 hours post-DTB release is the optimal time for nocodazole to enrich cells in G2/M in 6 hours.

10. Even though the DTB approach, alone or together with nocodazole treatment, can be used effectively for the enrichment of the S or G2/M phases of T47D cells, enrichment of the G1 phase requires approaches other than DTB, such as the CD-FBS approach. This indicates the use of more than one method for the enrichment of different phases of T47D cells, unlike MCF7 cells where the CD-FBS method combined with E2 supplementation and nocodazole treatment is sufficient for the enrichment of the G1, S, and G2/M phases.

Therefore, cell cycle phase enrichment of T47D cells may require optimization of other approaches.

As a summary, we found, among the various approaches used for cell cycle synchronization, CD-FBS and DTB methods, alone or in combination with nocodazole treatment, to be effective for cell cycle synchronizations and synchronization-coupled cell cycle phase enrichments of MCF7 and T47D cells. These approaches can be optimized and utilized for other cell lines based on their receptor expression status. However, it should be noted that cell lines with remarkably distinct molecular and phenotypic features may require tailored protocols for the enrichment of cell cycle phases.

REFERENCES

1. Global Cancer Observatory. *World Population Factsheet*. https://gco.iarc.who.int/media/globocan/factsheets/populations/900-world-fact-sheet.pdf (2022).

2. American Cancer Society. *Breast Cancer Facts & Figures 2022-2024*. https://www.cancer.org/content/dam/cancer-org/research/cancer-facts-and-statistics/breast-cancer-facts-and-figures/2022-2024-breast-cancer-fact-figures-acs.pdf (2022).

3. T.C. Sağlık Bakanlığı Halk Sağlığı Genel Müdürlüğü Kanser Dairesi Başkanlığı. Kanser Taramaları. https://hsgm.saglik.gov.tr/tr/kanser-taramalari.

4. Global Cancer Observatory. *Türkiye Factsheet*. https://gco.iarc.who.int/media/globocan/factsheets/populations/792-turkiye-fact-sheet.pdf (2022).

5. Guo, L. *et al.* Breast cancer heterogeneity and its implication in personalized precision therapy. *Experimental Hematology and Oncology* vol. 12 Preprint at https://doi.org/10.1186/s40164-022-00363-1 (2023).

6. Dawson, S. J., Rueda, O. M., Aparicio, S. & Caldas, C. A new genome-driven integrated classification of breast cancer and its implications. *EMBO Journal* vol. 32 Preprint at https://doi.org/10.1038/emboj.2013.19 (2013).

7. Holliday, D. L. & Speirs, V. Choosing the right cell line for breast cancer research. *Breast Cancer Research* vol. 13 Preprint at https://doi.org/10.1186/bcr2889 (2011).

8. Eroles, P., Bosch, A., Alejandro Pérez-Fidalgo, J. & Lluch, A. Molecular biology in breast cancer: Intrinsic subtypes and signaling pathways. *Cancer*

Treatment Reviews vol. 38 Preprint at https://doi.org/10.1016/j.ctrv.2011.11.005 (2012).

9. Soule, H. D., Vazquez, J., Long, A., Albert, S. & Brennan, M. A human cell line from a pleural effusion derived from a breast carcinoma1,2. *J Natl Cancer Inst* **51**, (1973).

10. Keydar, I. *et al.* Establishment and characterization of a cell line of human breast carcinoma origin. *European Journal of Cancer (1965)* **15**, (1979).

11. Lacroix, M. & Leclercq, G. Relevance of breast cancer cell lines as models for breast tumours: An update. *Breast Cancer Research and Treatment* vol. 83 Preprint at https://doi.org/10.1023/B:BREA.0000014042.54925.cc (2004).

12. Aka, J. A. & Lin, S. X. Comparison of functional proteomic analyses of human breast cancer cell lines T47D and MCF7. *PLoS One* **7**, (2012).

13. Radde, B. N. *et al.* Bioenergetic differences between MCF-7 and T47D breast cancer cells and their regulation by oestradiol and tamoxifen. *Biochemical Journal* **465**, (2015).

14. Smith, S. E. *et al.* Molecular characterization of breast cancer cell lines through multiple omic approaches. *Breast Cancer Research* **19**, (2017).

15. Saha, T., Makar, S., Swetha, R., Gutti, G. & Singh, S. K. Estrogen signaling: An emanating therapeutic target for breast cancer treatment. *European Journal of Medicinal Chemistry* vol. 177 Preprint at https://doi.org/10.1016/j.ejmech.2019.05.023 (2019).

16. Yaşar, P., Ayaz, G., User, S. D., Güpür, G. & Muyan, M. Molecular mechanism of estrogen–estrogen receptor signaling. *Reproductive Medicine and Biology* vol. 16 Preprint at https://doi.org/10.1002/rmb2.12006 (2017).

17. Huang, Y., Li, X. & Muyan, M. Estrogen receptors similarly mediate the effects of 17β-estradiol on cellular responses but differ in their potencies. *Endocrine* **39**, (2011).

18. Deroo, B. J. & Korach, K. S. Estrogen receptors and human disease. *Journal of Clinical Investigation* vol. 116 Preprint at https://doi.org/10.1172/JCI27987 (2006).

19. Huang, J. *et al.* Binding of estrogen receptor β to estrogen response element in Situ is independent of estradiol and impaired by its amino terminus. *Molecular Endocrinology* **19**, (2005).

20. Nott, S. L. *et al.* Genomic responses from the estrogen-responsive element-dependent signaling pathway mediated by estrogen receptor α are required to elicit cellular alterations. *Journal of Biological Chemistry* **284**, (2009).

21. Muyan, M., Callahan, L. M., Huang, Y. & Lee, A. J. The ligand-mediated nuclear mobility and interaction with estrogen-responsive elements of estrogen receptors are subtype specific. *J Mol Endocrinol* **49**, (2012).

22. Israels, E. D. & Israels, L. G. The cell cycle. *Oncologist* **5**, 510–513 (2000).

23. Caldon, C. E., Daly, R. J., Sutherland, R. L. & Musgrove, E. A. Cell cycle control in breast cancer cells. *Journal of Cellular Biochemistry* vol. 97 Preprint at https://doi.org/10.1002/jcb.20690 (2006).

24. Matthews, H. K., Bertoli, C. & de Bruin, R. A. M. Cell cycle control in cancer. *Nature Reviews Molecular Cell Biology* vol. 23 74–88 Preprint at https://doi.org/10.1038/s41580-021-00404-3 (2022).

25. May, K. M. & Hardwick, K. G. The spindle checkpoint. *J Cell Sci* **119**, (2006).

26. Davis, P. K., Ho, A. & Dowdy, S. F. Biological methods for cell-cycle synchronization of mammalian cells. *BioTechniques* vol. 30 Preprint at https://doi.org/10.2144/01306rv01 (2001).

27. Ligasová, A. & Koberna, K. Strengths and weaknesses of cell synchronization protocols based on inhibition of DNA synthesis. *International Journal of Molecular Sciences* vol. 22 Preprint at https://doi.org/10.3390/ijms221910759 (2021).

28. Eastman, A. E. & Guo, S. The palette of techniques for cell cycle analysis. *FEBS Letters* vol. 594 Preprint at https://doi.org/10.1002/1873-3468.13842 (2020).

29. Chen, G. & Deng, X. Cell synchronization by double thymidine block. *Bio Protoc* **8**, (2018).

30. Ikegami, S. *et al.* Aphidicolin prevents mitotic cell division by interfering with the activity of DNA polymerase-α [18]. *Nature* vol. 275 Preprint at https://doi.org/10.1038/275458a0 (1978).

31. Prall, O. W. J., Rogan, E. M. & Sutherland, R. L. Estrogen regulation of cell cycle progression in breast cancer cells. in *Journal of Steroid Biochemistry and Molecular Biology* vol. 65 (1998).

32. Sikora, M. J., Johnson, M. D., Lee, A. V. & Oesterreich, S. Endocrine response phenotypes are altered by charcoal-stripped serum variability. *Endocrinology* **157**, (2016).

33. Dalvai, M. & Bystricky, K. Cell cycle and anti-estrogen effects synergize to regulate cell proliferation and ER target gene expression. *PLoS One* **5**, (2010).

34. Gstraunthaler, G., Lindl, T. & Van Der Valk, J. A plea to reduce or replace fetal bovine serum in cell culture media. *Cytotechnology* vol. 65 Preprint at https://doi.org/10.1007/s10616-013-9633-8 (2013).

35. Frederiksen, H. *et al.* Sex-specific estrogen levels and reference intervals from infancy to late adulthood determined by LC-MS/MS. *Journal of Clinical Endocrinology and Metabolism* **105**, (2020).

36. Jordan, V. C. & Morrow, M. Tamoxifen, raloxifene, and the prevention of breast cancer. *Endocrine Reviews* vol. 20 Preprint at https://doi.org/10.1210/er.20.3.253 (1999).

37. Robertson, J. F. R. ICI 182,780 (Fulvestrant™) - The first oestrogen receptor down-regulator - Current clinical data. *Br J Cancer* **85**, (2001).

38. Demiralay, Ö. D. Cell cycle-dependent regulation of CXXC5 synthesis. (Middle East Technical University, 2022).

39. Zhu, H. *et al.* Induction of S-phase arrest and p21 overexpression by a small molecule 2[[3-(2,3-dichlorophenoxy)propyl]amino]ethanol in correlation with activation of ERK. *Oncogene* **23**, (2004).

40. Bustin, S. A. *et al.* The MIQE guidelines: Minimum information for publication of quantitative real-time PCR experiments. *Clin Chem* **55**, (2009).

41. Berry, M., Nunez, A. M. & Chambon, P. Estrogen-responsive element of the human pS2 gene is an imperfectly palindromic sequence. *Proc Natl Acad Sci U S A* **86**, (1989).

42. Lyng, M. B., Lænkholm, A. V., Pallisgaard, N. & Ditzel, H. J. Identification of genes for normalization of real-time RT-PCR data in breast carcinomas. *BMC Cancer* **8**, (2008).

43. Fleige, S. *et al.* Comparison of relative mRNA quantification models and the impact of RNA integrity in quantitative real-time RT-PCR. *Biotechnol Lett* **28**, (2006).

44. van der Valk, J. Fetal bovine serum—a cell culture dilemma. *Science* vol. 375 Preprint at https://doi.org/10.1126/science.abm1317 (2022).

45. Lee, D. Y. *et al.* Review of the current research on fetal bovine serum and the development of cultured meat. *Food Science of Animal Resources* vol. 42 Preprint at https://doi.org/10.5851/kosfa.2022.e46 (2022).

46. Cao, Z. *et al.* Effects of resin or charcoal treatment on fetal bovine serum and bovine calf serum. *Endocr Res* **34**, (2009).

47. Soto, A. M. & Sonnenschein, C. The role of estrogens on the proliferation of human breast tumor cells (MCF-7). *J Steroid Biochem* **23**, (1985).

48. Yu, H. & Yao, X. Cyclin B1: Conductor of mitotic symphony orchestra. *Cell Res* **18**, (2008).

49. Hwang, H. C. & Clurman, B. E. Cyclin E in normal and neoplastic cell cycles. *Oncogene* vol. 24 Preprint at https://doi.org/10.1038/sj.onc.1208613 (2005).

50. Wijayaratne, A. L. & McDonnell, D. P. The human estrogen receptor-α is a ubiquitinated protein whose stability is affected differentially by agonists, antagonists, and selective estrogen receptor modulators. *Journal of Biological Chemistry* **276**, (2001).

51. Alarid, E. T., Bakopoulos, N. & Solodin, N. Proteasome-mediated proteolysis of estrogen receptor: A novel component in autologous down-regulation. *Molecular Endocrinology* **13**, (1999).

52. Fan, M., Bigsby, R. M. & Nephew, K. P. The NEDD8 pathway is required for proteasome-mediated degradation of human estrogen receptor (ER)-α and essential for the antiproliferative activity of ICI 182,780 in ERα-positive breast cancer cells. *Molecular Endocrinology* **17**, (2003).

53. McDonnell, D. P. & Wardell, S. E. The molecular mechanisms underlying the pharmacological actions of ER modulators: Implications for new drug discovery in breast cancer. *Current Opinion in Pharmacology* vol. 10 Preprint at https://doi.org/10.1016/j.coph.2010.09.007 (2010).

54. Jordan, V. C. & O'Malley, B. W. Selective estrogen-receptor modulators and antihormonal resistance in breast cancer. *Journal of Clinical Oncology* vol. 25 Preprint at https://doi.org/10.1200/JCO.2007.11.3886 (2007).

55. Brzozowski, A. M. *et al.* Molecular basis of agonism and antagonism in the oestrogen receptor. *Nature* **389**, (1997).

56. Shiau, A. K. *et al.* The structural basis of estrogen receptor/coactivator recognition and the antagonism of this interaction by tamoxifen. *Cell* **95**, (1998).

57. Keyomarsi, K., Sandoval, L., Band, V. & Pardee, A. B. Synchronization of tumor and normal cells from G1 to multiple cell cycles by lovastatin. *Cancer Res* **51**, (1991).

58. Hengst, L., Dulic, V., Slingerland, J. M., Lees, E. & Reed, S. I. A cell cycle-regulated inhibitor of cyclin-dependent kinases. *Proc Natl Acad Sci U S A* **91**, (1994).

59. Rao, S. *et al.* Lovastatin-mediated G1 arrest is through inhibition of the proteasome, independent of hydroxymethyl glutaryl-CoA reductase. *Proc Natl Acad Sci U S A* **96**, (1999).

60. Moghadam-Kamrani, S. J. & Keyomarsi, K. Synchronization of the cell cycle using lovastatin. *Cell Cycle* **7**, (2008).

61. Dijkwel, P. A. & Hamlin, J. L. Initiation of DNA replication in the dihydrofolate reductase locus Is confined to the early S period in CHO cells synchronized with the plant amino acid mimosine. *Mol Cell Biol* **12**, (1992).

62. Krude, T. Mimosine arrests proliferating human cells before onset of DNA replication in a dose-dependent manner. *Exp Cell Res* **247**, (1999).

63. Galavazi, G., Schenk, H. & Bootsma, D. Synchronization of mammalian cells in vitro by inhibition of the DNA synthesis. I. Optimal conditions. *Exp Cell Res* **41**, (1966).

64. Galavazi, G. & Bootsma, D. Synchronization of mammalian cells in vitro by inhibition of the DNA synthesis. II. Population dynamics. *Exp Cell Res* **41**, (1966).

65. Galgano, P. J. & Schildkraut, C. L. G1/S phase synchronization using double thymidine synchronization. *Cold Spring Harb Protoc* **2006**, (2006).

66. Lee, J. & Gollahon, L. Mitotic perturbations induced by Nek2 overexpression require interaction with TRF1 in breast cancer cells. *Cell Cycle* **12**, (2013).

67. Osborne, C. K., Boldt, D. H. & Estrada, P. Human breast cancer cell cycle synchronization by estrogens and antiestrogens in culture. *Cancer Res* **44**, (1984).

68. Wakeling, A. E., Newboult, E. & Peters, S. W. Effects of antioestrogens on the proliferation of MCF-7 human breast cancer cells. *J Mol Endocrinol* **2**, (1989).

69. Butler, W. B. & Kelsey, W. H. Effects of tamoxifen and 4-hydroxytamoxifen on synchronized cultures of the human breast cancer cell line MCF-7. *Breast Cancer Res Treat* **11**, (1988).

70. Lykkesfeldt, A. E., Larsen, J. K., Christensen, I. J. & Briand, P. Effects of the antioestrogen tamoxifen on the cell cycle kinetics of the human breast cancer cell line, MCF-7. *Br J Cancer* **49**, (1984).

71. Carroll, J. S., Prall, O. W. J., Musgrove, E. A. & Sutherland, R. L. A pure estrogen antagonist inhibits cyclin E-Cdk2 activity in MCF-7 breast cancer cells and induces accumulation of p130-E2F4 complexes characteristic of quiescence. *Journal of Biological Chemistry* **275**, (2000).

72. Scholzen, T. & Gerdes, J. The Ki-67 protein: From the known and the unknown. *Journal of Cellular Physiology* vol. 182 Preprint at https://doi.org/10.1002/(SICI)1097-4652(200003)182:3<311::AID-JCP1>3.0.CO;2-9 (2000).

73. Beresford, M. J., Wilson, G. D. & Makris, A. Measuring proliferation in breast cancer: Practicalities and applications. *Breast Cancer Research* vol. 8 Preprint at https://doi.org/10.1186/bcr1618 (2006).

74. Bai, B. *et al.* Small molecule 2,3-DCPE induces S phase arrest by activating the ATM/ATR-Chk1-Cdc25A signaling pathway in DLD-1 colon cancer cells. *Oncol Lett* **20**, (2020).

75. Jordan, M. A., Thrower, D. & Wilson, L. Effects of vinblastine, podophyllotoxin and nocodazole on mitotic spindles Implications for the role of microtubule dynamics in mitosis. *J Cell Sci* **102**, (1992).

76. Schorl, C. & Sedivy, J. M. Analysis of cell cycle phases and progression in cultured mammalian cells. *Methods* **41**, (2007).

77. Dai, X., Cheng, H., Bai, Z. & Li, J. Breast cancer cell line classification and Its relevance with breast tumor subtyping. *Journal of Cancer* vol. 8 Preprint at https://doi.org/10.7150/jca.18457 (2017).

78. Rakha, E. A., Tse, G. M. & Quinn, C. M. An update on the pathological classification of breast cancer. *Histopathology* vol. 82 Preprint at https://doi.org/10.1111/his.14786 (2023).

79. Neve, R. M. *et al.* A collection of breast cancer cell lines for the study of functionally distinct cancer subtypes. *Cancer Cell* **10**, (2006).

80. Weigelt, B., Geyer, F. C. & Reis-Filho, J. S. Histological types of breast cancer: How special are they? *Molecular Oncology* vol. 4 Preprint at https://doi.org/10.1016/j.molonc.2010.04.004 (2010).

81. Huang, J., Li, X., Hilf, R., Bambara, R. A. & Muyan, M. Molecular basis of therapeutic strategies for breast cancer. *Current Drug Targets: Immune, Endocrine and Metabolic Disorders* vol. 5 Preprint at https://doi.org/10.2174/156800805774912944 (2005).

82. Osborne, C. K., Hobbs, K. & Trent, J. M. Biological differences among MCF-7 human breast cancer cell lines from different laboratories. *Breast Cancer Res Treat* **9**, (1987).

83. Burdall, S. E., Hanby, A. M., Lansdown, M. R. J. & Speirs, V. Breast cancer cell lines: Friend or foe? *Breast Cancer Research* vol. 5 Preprint at https://doi.org/10.1186/bcr577 (2003).

84. Kao, J. *et al.* Molecular profiling of breast cancer cell lines defines relevant tumor models and provides a resource for cancer gene discovery. *PLoS One* **4**, (2009).

APPENDICES

A. Supplementary Data

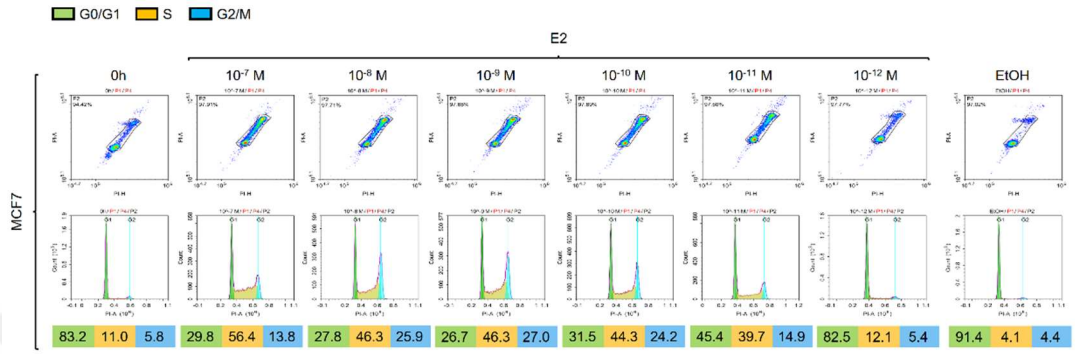

Figure 12. Effects of various concentrations of E2 on cycle progression of MCF7 cells synchronized at G0/G1. MCF7 cells grown in DMEM medium supplemented with 10% CD-FBS for 72h were either collected by trypsinization (0h) or treated without (0.01% ethanol, EtOH) or with various concentrations of (10^{-12} to 10^{-7} M) E2 for 24h in the same medium. Cells were then collected and subjected to flow cytometry analysis. G0/G1, S, and G2/M indicate cell cycle phases. Representative images with cell cycle phases from the same experiment are presented.

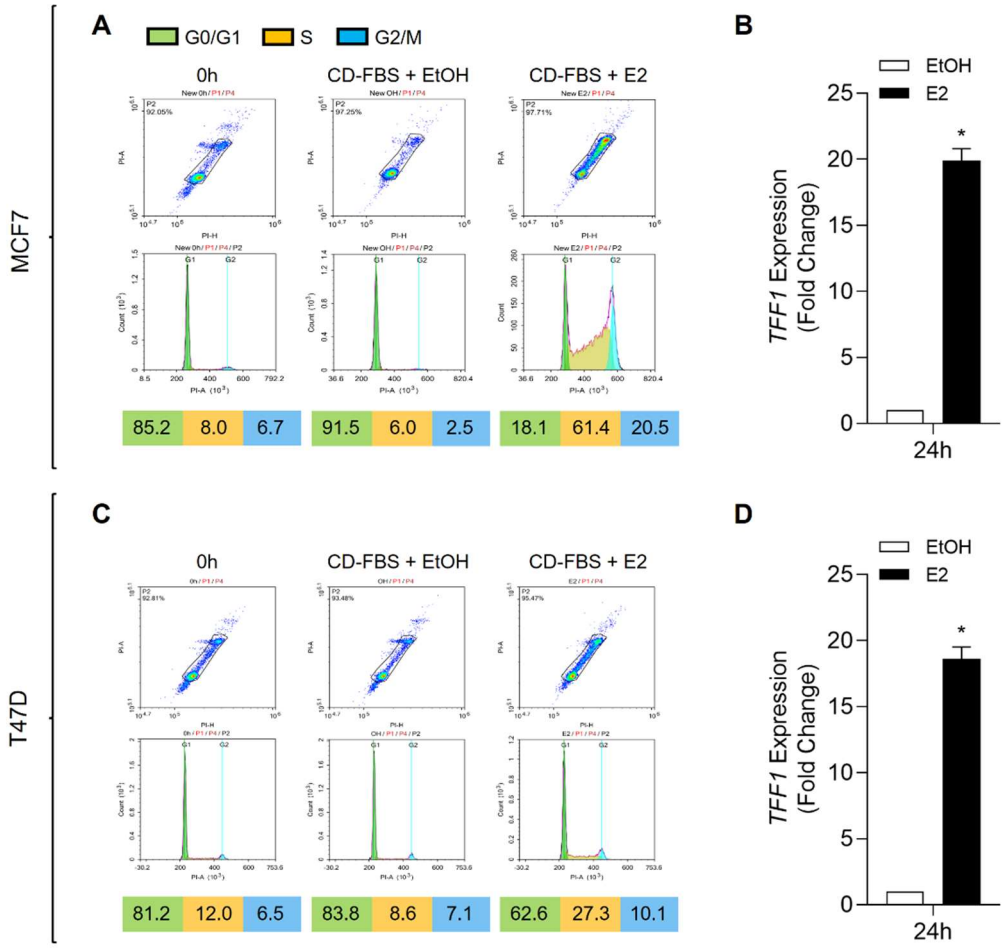

Figure 13. Effects of CD treatment of FBS, and E2 replacement on accumulation at G0/G1 and cycle progression of MCF7 and T47D cells. To examine the effects of CD-FBS on the accumulation of cells at G0/G1, **(A & B)** MCF7 or **(C & D)** T47D cells were grown in DMEM or RPMI 1640 medium, respectively, supplemented with 10% CD-FBS in 6-well tissue culture plates for 72h. Cells were either collected by trypsinization (0h) or treated without (0.01% ethanol, EtOH) or with 10^{-9} M E2 for 24h. **(A & C)** A fraction of the collected cells was subjected to flow cytometry, **(B & D)** and the remaining fraction was subjected to RNA isolation followed by RT-qPCR for the expression of *TFF1* using the expression of *RPL0* for normalization. RT-qPCR was performed for three biological replicates with three technical replicates for each. * represents significant changes ($P<0.05$; One-tailed, paired t-test with 95% confidence interval) in response to E2 compared to EtOH control. G0/G1, S, and G2/M indicate cell cycle phases.

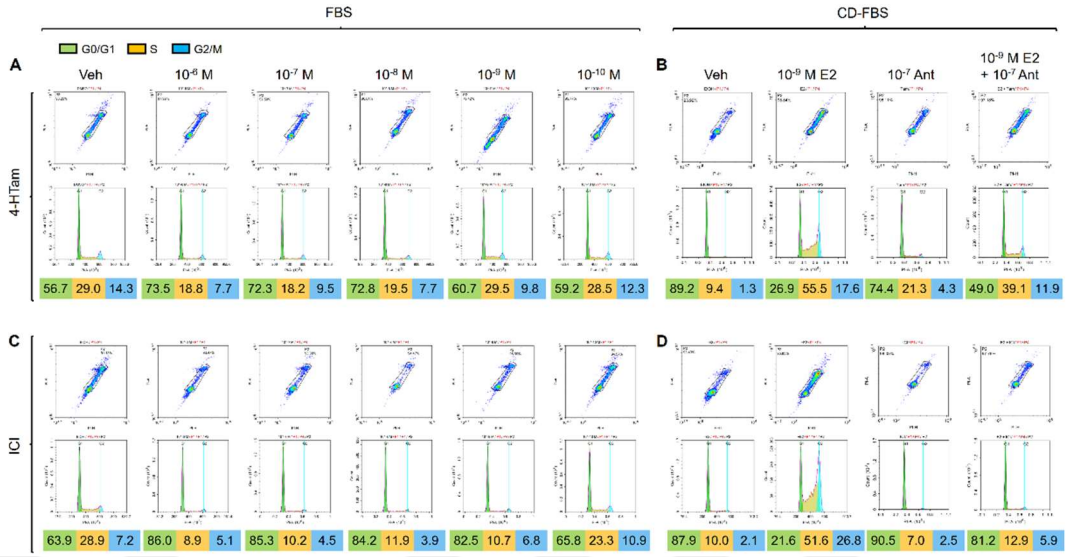

Figure 14. Effects of 4-hydroxytamoxifen, 4-HTam, or Imperial Chemical Industries 182780, ICI, on cycle phase distribution of MCF7 cells. (A & C) Cells maintained in DMEM medium supplemented with 10% FBS were incubated in fresh media containing 0.0002% DMSO or 0.01% ethanol as the vehicle (Veh) control respectively, or various concentrations, 10^{-10} to 10^{-6} M **(A)** 4-HTam or **(C)** ICI for 24h. Cells were collected by trypsinization and subjected to flow cytometry. **(B & D)** MCF7 cells maintained in DMEM medium supplemented with 10% CD-FBS for 72h to synchronize cells at G0/G1 were incubated in the same medium without (Veh) or with E2 (10^{-9} M) and/or **(B)** 4-HTam (10^{-7} M) or **(D)** ICI (10^{-7} M) for 24h. Cells were then collected and subjected to flow cytometry analysis. G0/G1, S, and G2/M indicate cell cycle phases. Representative images with cell cycle phases from the same experiment are presented.

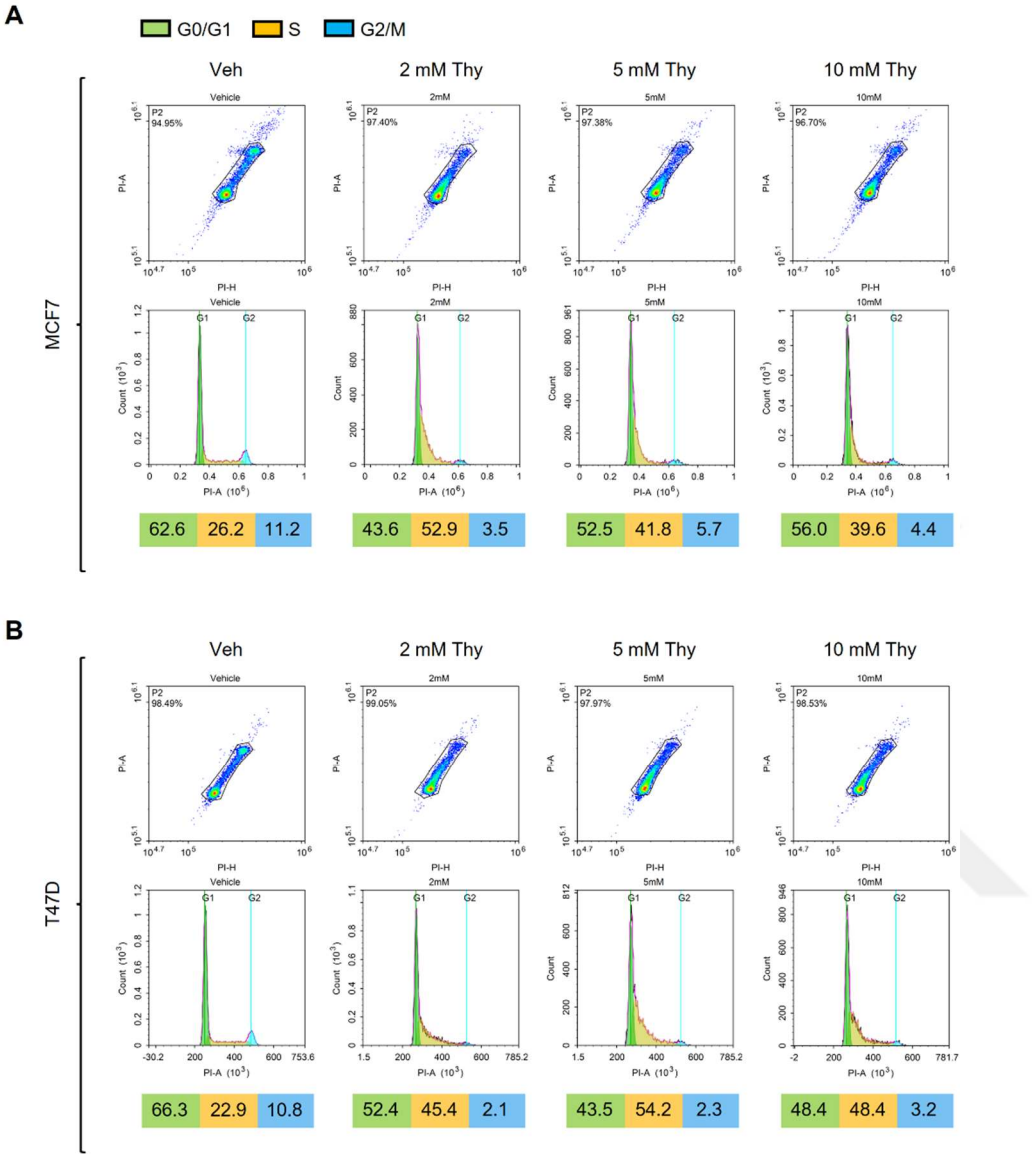

Figure 15. Effects of various concentrations of thymidine (Thy) on cycle synchronization of MCF7 and T47D cells. (A) MCF7 or **(B)** T47D cells maintained in DMEM or RPMI 1640 medium, respectively, supplemented with 10% FBS were incubated in fresh media with vehicle control (Veh) or various concentrations (2, 5, or 10 mM) of thymidine for 14h. Cells were then released from thymidine treatment by washing the cells with 1x PBS and re-incubating them in their respective medium containing 10% FBS without thymidine for 12h. The cells were subsequently washed and incubated with the same medium containing 10% FBS and vehicle control (Veh) or 2, 5, or 10 mM thymidine for 22h. Cells were collected with trypsinization and subjected to flow cytometry. G0/G1, S, and G2/M indicate cell cycle phases. Representative images from the same experiment are shown.

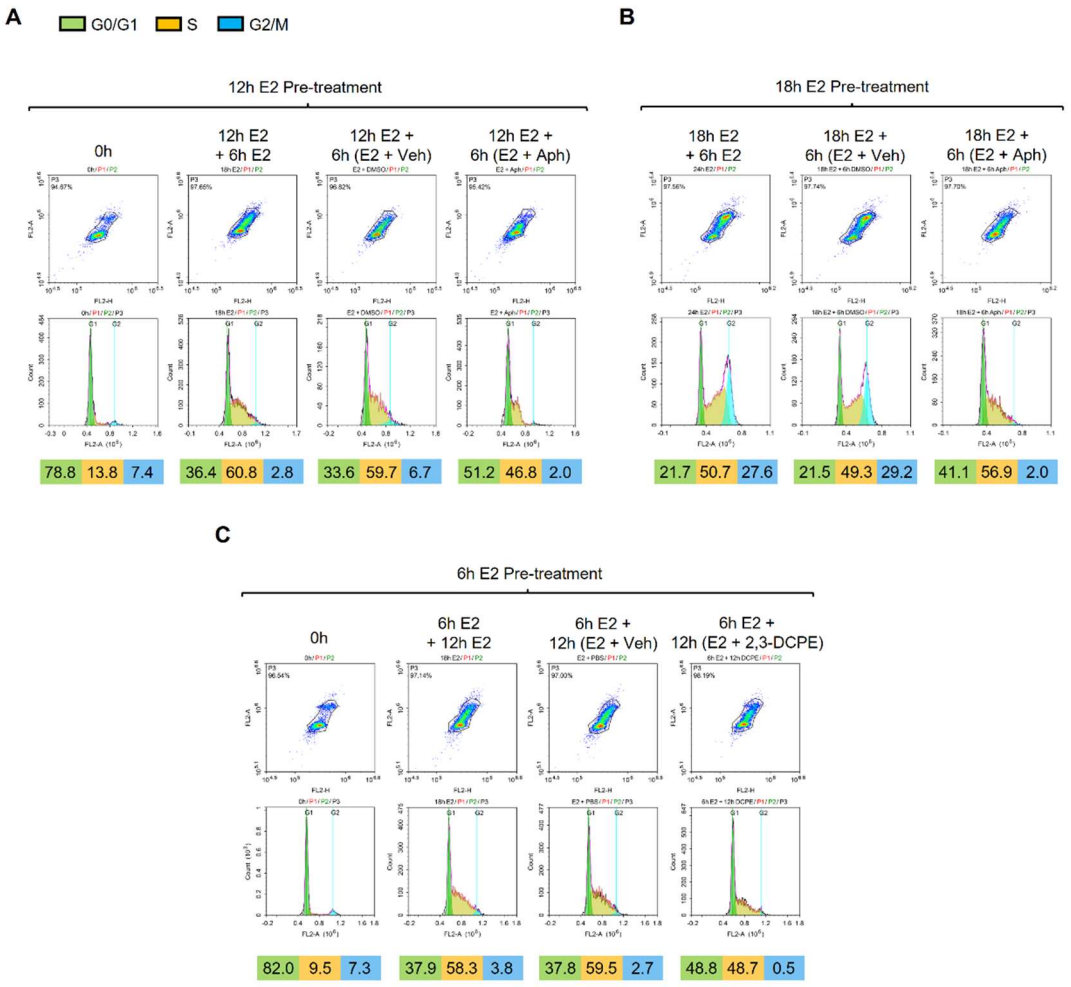

Figure 16. Determination of the optimal time for the enrichment of the S phase by aphidicolin (Aph) or 2,3-DCPE in synchronized MCF7 cells present at different stages of the S phase induced by the E2 treatment. (A & B) MCF7 cells grown in DMEM medium supplemented with 10% CD-FBS for 72h were either collected by trypsinization (0h) or treated in the same medium with 10^{-9} M E2 for **(A)** 12h, or **(B)** 18h. Cells were then incubated in the same medium without (0.01% DMSO as the vehicle control for aphidicolin) or with 10 µM aphidicolin in the absence or presence of 10^{-9} M E2 for an additional 6h. At the termination, cells were collected by trypsinization and subjected to flow cytometry. Representative images with cell cycle phases from the same experiment are presented. **(C)** MCF7 cells grown in DMEM medium supplemented with 10% CD-FBS for 72h were either collected by trypsinization (0h) or treated in the same medium with 10^{-9} M E2 for 6h and subsequently without (0.01% PBS as the vehicle control for 2,3-DCPE) or with 20 µM 2,3-DCPE in the absence or presence of 10^{-9} M E2 for an additional 12h. At the termination, cells were collected by trypsinization and subjected to flow cytometry. Representative images with cell cycle phases from the same experiment are presented.

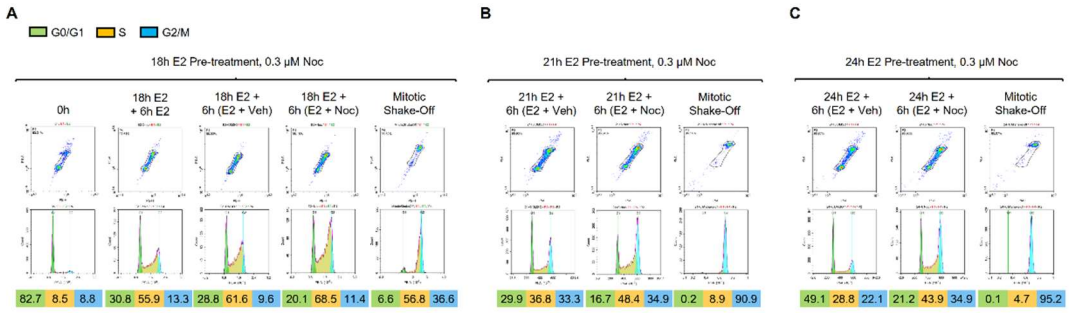

Figure 17. Assessing the optimal time for the enrichment of the G2/M or M phase by nocodazole (Noc) in synchronized MCF7 cells present at different stages of the S phase in response to the E2 treatment. MCF7 cells grown in DMEM medium supplemented with 10% CD-FBS for 72h were either collected by trypsinization (0h) or treated in the same medium with 10^{-9} M E2 for (**A**) 18h, (**B**) 21h, or (**C**) 24h. Cells were re-incubated in the fresh medium containing 10^{-9} M E2 and/or DMSO, as vehicle control for nocodazole, or 0.3 µM nocodazole (Noc) for an additional 6h. At the termination, cells were either subjected to trypsinization or mitotic shake-off for collection. The phase distribution of cells was assessed with the flow cytometer. Representative images with cell cycle phases from the same experiment are presented.

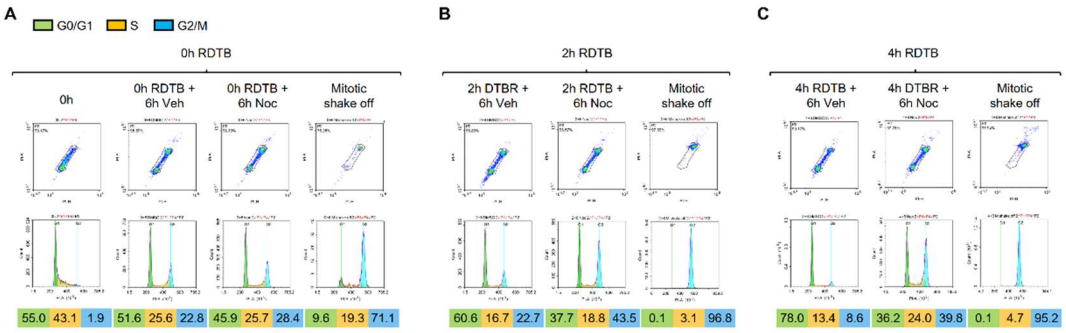

Figure 18. Examination of the optimal time for the enrichment of the G2/M or M phase by nocodazole (Noc) following the release of synchronized T47D cells from double thymidine block (RDTB). T47D cells grown in RPMI 1640 medium supplemented with 10% FBS were synchronized at the G1/S transition with 2 mM thymidine and released with fresh RPMI 1640 medium supplemented with 10% FBS. At the time of release (**A**) 0h, or (**B**) 2h, or (**C**) 4h after the release, the cells were treated without (0.01% DMSO) or with 0.3 µM nocodazole (Noc) for an additional 6h. At the termination, cells were either subjected to trypsinization or mitotic shake-off followed by flow cytometry for the phase distribution. Representative images with cell cycle phases from the same experiment are shown.

B. Primers

Table 4. Primer list

Primer Name	Sequence (5' – 3')
GAPDH_FP	GGGAGCCAAAAGGGTCATCA
GAPDH_REP	TTTCTAGACGGCAGGTCAGGT
pS2/TFF1_FP	TTGTGGTTTTCCTGGTGTCA
pS2/TFF1_REP	CCGAGCTCTGGGACTAATCA
RPLP0_FP	GGAGAAACTGCTGCCTCATA
RPLP0_REP	GAAAAAGGAGGTCTTCTCG

C. MIQE Checklist

Table 5. MIQE checklist

ITEM TO CHECK	IMPORTANCE	CHECKLIST
EXPERIMENTAL DESIGN		
Definition of experimental and control groups	**E**	YES
Number within each group	**E**	YES
Assay carried out by core lab or investigator's lab?	D	YES
Acknowledgement of authors' contributions	D	N/A
SAMPLE		
Description	**E**	N/A
Volume/mass of sample processed	D	N/A
Microdissection or macrodissection	**E**	N/A
Processing procedure	**E**	N/A
If frozen - how and how quickly?	**E**	N/A
If fixed - with what, how quickly?	**E**	N/A
Sample storage conditions and duration (especially for FFPE samples)	**E**	N/A
NUCLEIC ACID EXTRACTION		
Procedure and/or instrumentation	**E**	YES
Name of kit and details of any modifications	**E**	YES
Source of additional reagents used	D	N/A
Details of DNase or RNAse treatment	**E**	YES
Contamination assessment (DNA or RNA)	**E**	YES
Nucleic acid quantification	**E**	YES
Instrument and method	**E**	YES
Purity (A260/A280)	D	YES
Yield	D	YES
RNA integrity method/instrument	**E**	NO
RIN/RQI or Cq of 3' and 5' transcripts	**E**	NO
Electrophoresis traces	D	NO
Inhibition testing (Cq dilutions, spike or other)	**E**	NO
REVERSE TRANSCRIPTION		
Complete reaction conditions	**E**	YES
Amount of RNA and reaction volume	**E**	YES
Priming oligonucleotide (if using GSP) and concentration	**E**	YES

Table 5 (continued)

Reverse transcriptase and concentration	**E**	YES
Temperature and time	**E**	YES
Manufacturer of reagents and catalogue numbers	D	YES
Cqs with and without RT	D*	NO
Storage conditions of cDNA	D	YES
qPCR TARGET INFORMATION		
If multiplex, efficiency and LOD of each assay.	**E**	N/A
Sequence accession number	**E**	YES
Location of amplicon	D	YES
Amplicon length	**E**	YES
In silico specificity screen (BLAST, etc)	**E**	YES
Pseudogenes, retropseudogenes or other homologs?	D	YES
Sequence alignment	D	YES
Secondary structure analysis of amplicon	D	NO
Location of each primer by exon or intron (if applicable)	**E**	YES
What splice variants are targeted?	**E**	YES
qPCR OLIGONUCLEOTIDES		
Primer sequences	**E**	YES
RTPrimerDB Identification Number	D	N/A
Probe sequences	D**	N/A
Location and identity of any modifications	**E**	N/A
Manufacturer of oligonucleotides	D	YES
Purification method	D	YES
qPCR PROTOCOL		
Complete reaction conditions	**E**	YES
Reaction volume and amount of cDNA/DNA	**E**	N/A
Primer, (probe), Mg++ and dNTP concentrations	**E**	N/A
Polymerase identity and concentration	**E**	YES
Buffer/kit identity and manufacturer	**E**	YES
Exact chemical constitution of the buffer	D	YES
Additives (SYBR Green I, DMSO, etc.)	**E**	YES
Manufacturer of plates/tubes and catalog number	D	YES
Complete thermocycling parameters	**E**	YES
Reaction setup (manual/robotic)	D	YES
Manufacturer of qPCR instrument	**E**	YES
qPCR VALIDATION		
Evidence of optimisation (from gradients)	D	NO

Table 5 (continued)

Specificity (gel, sequence, melt, or digest)	**E**	YES
For SYBR Green I, Cq of the NTC	**E**	YES
Standard curves with slope and y-intercept	**E**	YES
PCR efficiency calculated from slope	**E**	YES
Confidence interval for PCR efficiency or standard error	D	NO
r2 of standard curve	**E**	YES
Linear dynamic range	**E**	YES
Cq variation at lower limit	**E**	YES
Confidence intervals throughout range	D	N/A
Evidence for limit of detection	**E**	NO
If multiplex, efficiency and LOD of each assay.	**E**	N/A
DATA ANALYSIS		
qPCR analysis program (source, version)	**E**	YES
Cq method determination	**E**	YES
Outlier identification and disposition	**E**	N/A
Results of NTCs	**E**	YES
Justification of number and choice of reference genes	**E**	YES
Description of normalisation method	**E**	YES
Number and concordance of biological replicates	D	YES
Number and stage (RT or qPCR) of technical replicates	**E**	YES
Repeatability (intra-assay variation)	E	YES
Reproducibility (inter-assay variation, %CV)	D	YES
Power analysis	D	NO
Statistical methods for result significance	**E**	YES
Software (source, version)	E	YES
Cq or raw data submission using RDML	**D**	N/A

E: essential information, D: desirable information, N/A: not applicable

D. Flow Cytometry Gating Strategy

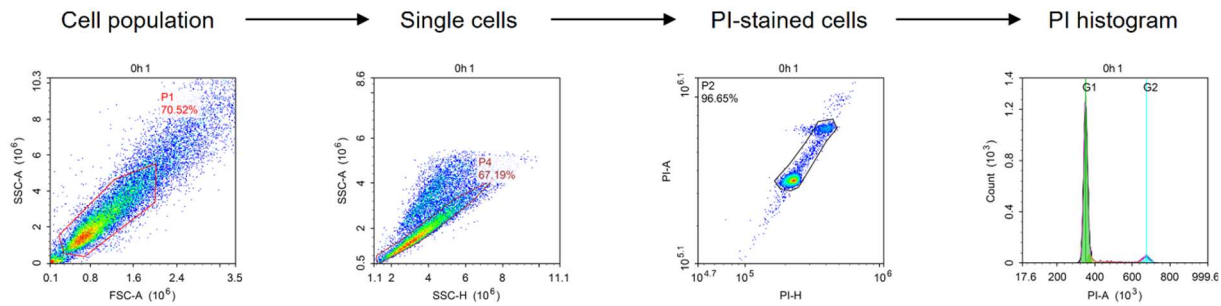

Figure 19. A sample gating strategy used for the flow cytometry analysis.

E. Buffers

RIPA Buffer

150 mM NaCl

5 mM EDTA, pH = 8.0

50 mM Tris, pH = 8.0

1% NP-40

0.5% Sodium deoxycholate

0.1% SDS

6x Laemmli Buffer

375 mM Tris, pH = 6.8

12% SDS

60% Glycerol

0.012% Bromophenol blue

β-mercaptoethanol is added freshly before use with a final concentration of 30%.